Superbasic Alkyl-Substituted Bisphosphazene Proton Sponges: Synthesis, Structural Features, Thermodynamic and Kinetic Basicity, Nucleophilicity and Coordination Chemistry

ARTICLE *in* CHEMISTRY - A EUROPEAN JOURNAL · JUNE 2014

Impact Factor: 5.73 · DOI: 10.1002/chem.201402226

7 AUTHORS, INCLUDING:

Xiulan Xie
Philipps University of Marburg
85 PUBLICATIONS **1,486** CITATIONS
SEE PROFILE

Eduard Baal
Philipps University of Marburg
1 PUBLICATION **4** CITATIONS
SEE PROFILE

Benjamin Oelkers
Technische Universität Kaiserslautern
22 PUBLICATIONS **126** CITATIONS
SEE PROFILE

Boris Kovacevic
Ruđer Bošković Institute
51 PUBLICATIONS **1,343** CITATIONS
SEE PROFILE

ChemPubSoc Europe

DOI: 10.1002/chem.201402226

CHEMISTRY A European Journal Full Paper

Phosphazenes

Superbasic Alkyl-Substituted Bisphosphazene Proton Sponges: Synthesis, Structural Features, Thermodynamic and Kinetic Basicity, Nucleophilicity and Coordination Chemistry

Julius F. Kögel,[a] Xiulan Xie,[a] Eduard Baal,[a] Donatas Gesevičius,[a] Benjamin Oelkers,[a] Borislav Kovačević,[b] and Jörg Sundermeyer*[a]

Dedicated to Professor Helmut Werner, Würzburg, on the occasion of his 80th birthday

Abstract: Herein we describe an easily accessible class of superbasic proton sponges based on the 1,8-bisphosphazenylnaphthalene (PN) proton pincer motif and P-alkyl substituents ranging from methyl (TMPN) to *n*-butyl (TBPN), isopropyl (TiPrPN) and cyclopentyl (TcyPPN). These neutral bases with a pK_{BH}^{+} value (MeCN) of ~30 were accessible via a Kirsanov condensation using commercially available 1,8-diaminonaphthalene, and in case of TMPN and TBPN, simple one-pot procedures starting from trisalkylphosphanes can be performed. Furthermore, the known pyrrolidinyl-substituted superbase TPPN previously synthesized via a Staudinger reaction could also be prepared by the Kirsanov strategy allowing its preparation in a larger scale. The four alkyl-substituted proton sponges were structurally characterized in their protonated form; molecular XRD structures were also obtained for unprotonated TiPrPN and TcyPPN. Moreover, we present a detailed description of spectroscopic features of chelating bisphosphazenes including TPPN and its hyperbasic homologue P_2-TPPN on which we reported recently. The four alkyl-substituted superbases were investigated with respect to their basic features by computational means and by NMR titration experiments revealing unexpectedly high experimental pK_{BH}^{+} values in acetonitrile between 29.3 for TMPN and 30.9 for TBPN. Besides their thermodynamic basicity, we exemplarily studied the kinetic basicity of TMPN and TPPN by means of NMR-spectroscopic methods. Furthermore, the competing nucleophilic versus basic properties were examined by reacting the proton sponges with ethyl iodide. Insight into the coordination chemistry of chelating superbases was provided by reacting TMPN with trimethylaluminum and trimethylgallium to give cationic complexes of Group XIII metal alkyls that were structurally characterized.

Introduction

The first proton sponge was discovered in the late 1960s by Alder, who noticed the unexpectedly high basicity of 1,8-bis(dimethylamino)naphthalene (DMAN).[1] DMAN exhibits a pK_{BH}^{+} value of 12.34 in water and surprisingly outnumbers the corresponding values of other aromatic amines such as *N*,*N*-dimethylaniline ($pK_{BH}^{+}(H_2O) = 5.06$)[2] or the non-alkylated analog 1,8-diaminonaphthalene ($pK_{BH}^{+}(H_2O) = 4.61$)[1] by more than seven orders of magnitude. Successive methylation of the latter compound lead to an abrupt rise in basicity after introduction of the fourth alkyl group. This phenomenon originates from the spatial proximity of the two basicity centers in *peri*-position and the repulsion of their lone pairs leading to the unfavorable distortion of the naphthalene backbone in the proton sponge's free base form. The situation changes after protonation: An intramolecular hydrogen bridge is formed allowing relaxation of the aromatic spacer. The term proton sponge can be referred to the low kinetic basicity of most representatives of this class. The hydrophobic shielding of the basicity centers provided by DMAN's alkyl groups causes a very low proton self-exchange rate which limits the proton sponges' potential to act as bases in catalytic applications.

Naphthalene-based proton sponges, in particular the commercially available 1,8-dimethylamino and tetramethy-guanidino derivatives, DMAN and TMGN, have found various applications as versatile nonionic bases in organic synthesis.[3–8] Furthermore, they are interesting model compounds for the experimental and theoretical investigation of proton exchange barriers and the geometry of [N-H···N] hydrogen bonds that play an important role in biological systems.[9] The combination of proton sponges with strong Lewis acids leads to frustrated Lewis pairs which are able to activate molecular hydrogen by heterolytic cleavage.[10] Guanidinyl-substituted proton sponges

[a] J. F. Kögel, Dr. X. Xie, E. Baal, D. Gesevičius, Dr. B. Oelkers, Prof. Dr. J. Sundermeyer
Fachbereich Chemie
Philipps-Universität Marburg
Hans-Meerwein-Straße, 35032 Marburg (Germany)
Fax: (+49) 642128-25711
E-mail: jsu@staff.uni-marburg.de

[b] Dr. B. Kovačević
Quantum Chemistry Group
Rudjer Bošković Institute
Bijenička c. 54, 10000 Zagreb (Croatia)

Supporting information for this article is available on the WWW under http://dx.doi.org/10.1002/chem.201402226.

can act as chelate ligands for main group and transition metals.[11] For DMAN various additional applications are known such as the use as a matrix in MALDI mass spectrometry,[12] as a solid-phase extractor for perfluoroalkyl sulfonates after immobilization on silica particles,[13] as a membrane in fuel cells[14] or as an antioxidant in lubricants.[15]

Having understood the nature of DMAN's high basicity, a large number of synthetic chemists have been engaged in the modification of Alder's classical proton sponge to further enhance its pK_{BH^+} value. One strategy is the attachment of electron-donating substituents to the naphthalene backbone. The so-called buttressing effect describes the substitution of the 2- and 7-position by preferably electron-rich and bulky groups further destabilizing the unprotonated proton sponge by enforcing an even stronger repulsion of the nitrogen atoms' lone pairs.[16] Another possible modification of naphthalene-based proton sponges is the variation of the substituents at the basicity centers. Besides the replacement of DMAN's methyl groups by numerous different alkyl substituents,[17–19] the nitrogen atoms have been integrated in an aromatic system as for instance shown in Staab's quino[7,8*h*]quinoline.[20] This structure motive was recently further modified by Shaffer et al.[21] Apart from varying the substituents of DMAN, several proton-chelating compounds with backbones other than naphthalene have been synthesized. The interaction of two basicity centers has also been achieved by aromatic spacers such as fluorene,[22] heterofluorene,[23] phenantrene,[24] biphenyl[25] or helicene[26] moieties. Potáček et al. reported on the preparation of caged proton sponges with a non-aromatic skeleton.[27] Recently, the basicity of macrocyclic amino compounds with interacting basicity centers was studied theoretically and experimentally.[28] Examples for literature known proton sponges are shown in Figure 1.

Whereas modifications at DMAN's aromatic backbone or the replacement of the methyl groups at the basicity centers by other alkyl substituents only lead to minor increases in the pK_{BH^+} value, an enormous basicity enhancement can be achieved by combining Alder's concept of interacting basicity centers with other building blocks with a high intrinsic basicity. A naphthalene-based proton sponge bearing two cyclopropeniminyl moieties was reported by Belding and Dudding quite recently.[29] The—for a long time—most basic proton sponge (pK_{BH^+}(MeCN) = 31.94) was a vinamidine compound reported by Schwesinger et al. bearing two interacting amidine units and exhibiting a high kinetic basicity.[30] Further proton sponges with a high proton self-exchange rate calling for application as proton transfer catalysts have been prepared in our group by connecting two guanidinyl moieties via a 1,8-disubstituted naphthalene skeleton.[31] Among them is the commercially available 1,8-bis(tetramethyl-guanidinyl)naphthalene (TMGN) (Figure 2). Such compounds have been further investigated by Himmel et al. concerning their coordination chemistry and electrochemical behavior.[11c—e] The combination of Alder's proton sponges with Schwesinger's concept of superbasic phosphazene bases[32] was achieved in 1,8-bis(hexamethyltriaminophosphazenyl)naphthalene (HMPN) which shows a pK_{BH^+} value of 29.9 in acetonitrile.[33] Recently, we have reported on the preparation of the two bisphosphazene proton sponges TPPN and its higher homologue P_2-TPPN via a Staudinger reaction.[34] The latter compound is the most basic representative of the class of proton sponges with a pK_{BH^+} value of 42.1 on the acetonitrile scale. Synthetic and computational efforts in the area of proton sponges and superbases in general have been summarized in several review articles by Staab, Alder, Llamas–Saiz, Maksić, Pozharskii, Chambron and Ishikawa.[3,35]

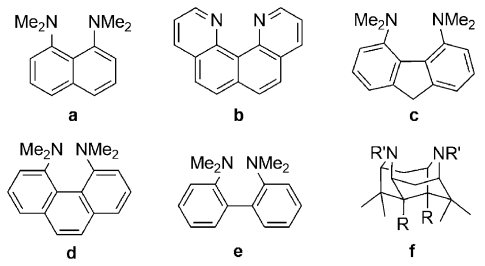

Figure 1. Alder's proton sponge DMAN (a) [1]and aromatic sponges with quino[7,8-*h*]quinoline (b),[20] fluorene (c),[22] phenantrene (d)[24] and biphenyl (e)[25] backbones as well as a proton sponge with a non-aromatic skeleton.[27]

Naphthalene-based bisphosphazene proton sponges with alkyl or aryl substituents at the phosphorus atoms that are the main topic of this publication were reported by Llamas–Saiz et al. in the early 1990s for the first time. Two representatives bearing PPh_3 and PPh_2Me moieties were characterized in their protonated forms, but exhibited only a moderate pK_{BH^+} value of 15.6 in water in case of the triphenylphosphane-substituted species due to the electron-withdrawing effect of the aryl substituents.[36] 1,8-Bis[tributylphosphazenyl]naphthalene (TBPN) that is also treated herein first appeared in literature in 2008, but apparently its protonated form was obtained and mistaken for the free base.[37] A preliminary communication on the syn-

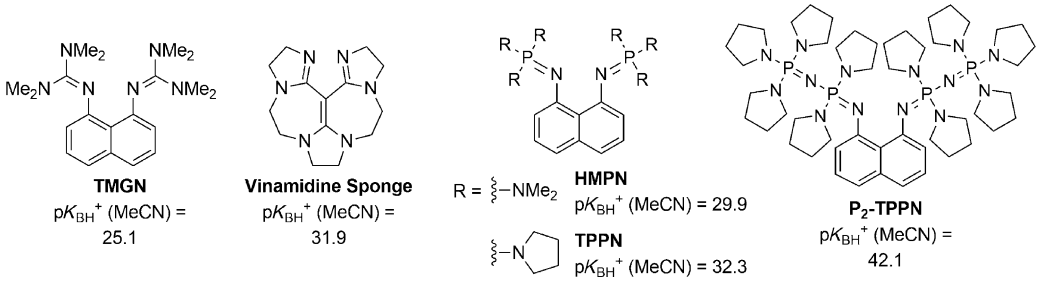

Figure 2. Hybrid superbases with guanidine,[31a] amidine[30] and phosphazene moieties.[33,34]

thesis and properties of TBPN and other members of this class of superbases appeared in 2011.[38] Recently, Driess et al. published the synthesis of TBPN using it for the stabilization of silyliumylidene $[ClSi:]^+$ and the silathionium $[ClSi{=}S]^+$ cations.[39]

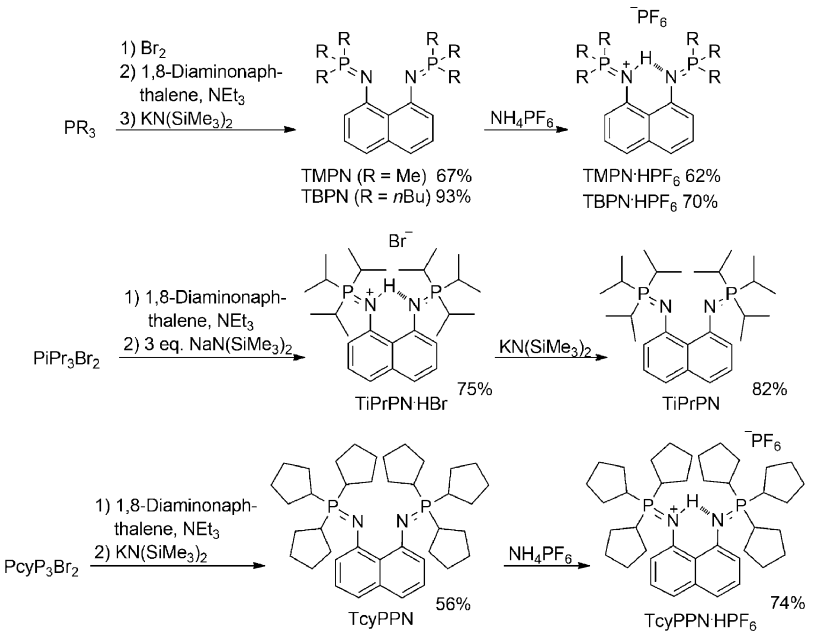

Scheme 1. Preparation of TMPN, TBPN; TiPrPN and TcyPPN via the Kirsanov reaction.

Results and Discussion

Synthesis

The Staudinger[40] and the Kirsanov reaction[41] are the two most prominent synthetic tools for the formation of phosphorus nitrogen double or zwitterionic bonds of phosphazenes. Recently, we reported the synthesis of TPPN and P_2-TPPN via a Staudinger reaction,[34] but the general synthetic use of this procedure is not only limited by the surprisingly high stability of the initially formed bisphosphazides,[42] but also by the application of 1,8-diazidonaphthalene which is difficult to synthesize and can only be obtained in small quantities. In contrast, the Kirsanov reaction makes use of cheap commercially available 1,8-diaminonaphthalene. However, the scope of this strategy turned out to be limited by the spatial proximity of the two amino groups in 1,8-diaminonaphthalene: Whereas the Kirsanov reaction proceeds readily for simple aromatic amines such as aniline,[43] the synthesis of HMPN required extensive optimization of the reaction conditions and the proton sponge was only obtained in a moderate yield of 43%. Another drawback of the Kirsanov reaction is that the desired superbase is obtained in its protonated form and the free base has to be liberated in another reaction step. This can be difficult not only due to the high thermodynamic basicity, but especially because of the hydrophobic shielding of the acidic proton that is caught in a stable N-H···N hydrogen bridge. Hence, the Kirsanov reaction turned out to be unsuitable for most amino-substituted phosphorous compounds in the course of our investigations, but it was successful for the synthesis of the four alkyl-substituted bisphosphazene proton sponges presented herein.

The preparation of TMPN and TBPN (Scheme 1) proceeded readily in simple one-pot procedures starting from the corresponding phosphanes which were oxidized in situ by bromine in an aromatic solvent. Subsequently, a solution of 1,8-diaminonaphthalene and triethylamine was added at room temperature and the heterogeneous reaction mixtures were stirred upon heating. Triethylamine acted as an auxiliary base quenching liberated hydrogen bromide, but of course it is not basic enough to deprotonate the HBr salts of the proton sponges. The free bases of TMPN and TBPN were liberated by addition of $KN(SiMe_3)_2$. Their protonated forms were prepared in separate steps by reaction with NH_4PF_6.

Attempts to obtain TiPrPN via a one-pot procedure resulted in incomplete conversion and the formation of several side products which were detected via ^{31}P NMR spectroscopy of the reaction mixture. The more complicated synthesis can be referred to the higher steric demand of the secondary isopropyl groups compared to methyl or *n*-butyl substituents. Thus, we decided to split the three reaction steps. $[iPr_3PBr]^+Br^-$ was isolated and reacted with 1,8-diaminonaphthalene in presence of the auxiliary base triethylamine. ^{31}P NMR spectroscopic monitoring of the reaction progress still revealed the formation of side products. Finally, isolation of TiPrPN·HBr was achieved by adding three equivalents of $NaN(SiMe_3)_2$ deprotonating the less basic byproducts, but not the superbasic proton sponge and allowing separation due to the different solubility properties. The deprotonation of TiPrPN·HBr was performed in a separate step by $KN(SiMe_3)_2$ in toluene (Scheme 1). The synthesis of TcyPPN also started from the corresponding bromophosphonium bromide $[cyP_3PBr]^+Br^-$ ($cyP = -CH(CH_2)_4$), but deprotonation was achieved in situ by $KN(SiMe_3)_2$ (Scheme 1).

TPPN that was formerly accessible via a Staudinger reaction[34] could also be synthesized by the Kirsanov reaction allowing its preparation in large scale (Scheme 2).[44] Bromination of tris(pyrrolidinyl)phosphane and reaction with 1,8-diaminonaphthalene were performed in one-pot fashion yielding the proton sponge's hydrobromide. Deprotonation turned out to be difficult and in many cases mixtures of the free base and the hydrobromide were obtained. Among the tested bases such as metal hydrides, amides or organometallic compounds, the best deprotonation conditions were observed using $KN(SiMe_3)_2$ in hexane at 60 °C which yielded TPPN in 64%.

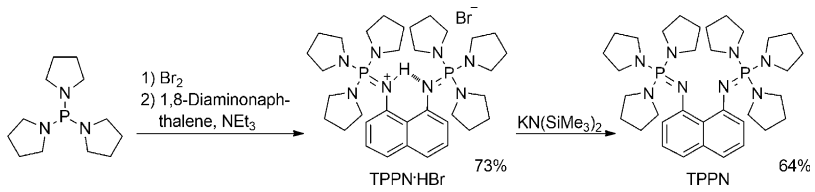

Scheme 2. Preparation of TPPN·HBr via the Kirsanov reaction and deprotonation by $KN(SiMe_3)_2$.

Spectroscopic Properties

^{31}P and ^{1}H NMR chemical shifts of the bisphosphazene proton sponges described herein are summarized in Table 1. Protonation led to a low-field shift of about 16 ppm for the ^{31}P NMR signals of the amino-substituted sponges HMPN and TPPN and more than 28 ppm in case of the alkyl-substituted species. The ^{1}H NMR signals of the aromatic protons are shifted towards the high field and their order is changed while those of the acidic protons in the protonated compounds exhibit considerable low-field shifts as described earlier for proton sponges. Thus, for the amino-substituted bisphosphazenes ^{1}H signals near 15 ppm were reported whereas for the alkyl-substituted sponges the ^{1}H resonance position varied from 13.32 ppm for TcyPPN·HBr to 15.84 ppm for TMPN·HPF_6. The acidic protons of TiPrPN·HBr ($\delta_{NH}=14.05$ ppm) and TcyPPN·HPF_6 ($\delta_{NH}=13.32$ ppm) are considerably shifted towards the high field compared to the other two alkyl-substituted bisphosphazenes studied herein. This high-field shift is accompanied by the observation that TiPrPN and TcyPPN show longer N···N distances (2.634(4) and 2.641(3) Å) in their protonated forms than found for TMPN (2.57(1) Å) and TBPN (2.594(4) Å) (see below). Even higher values for the chemical shifts of the acidic protons were observed by Llamaz–Saiz et al. for the hydrobromides of two bisphosphazene sponges bearing PPh_3 ($\delta_{NH}=16.42$ ppm, $^{2}J(P,H)=4.8$ Hz) and PPh_2Me ($\delta_{NH}=16.64$ ppm) moieties.[36b] The acidic proton in the hydrochloride of Alder's DMAN exhibits a value of 18.6 ppm in $[D_3]$MeCN.[35e] The effect of intramolecular hydrogen bonding on the proton NMR chemical shift of the acidic proton can be observed when comparing the corresponding value of P_2-TPPN (15.14 ppm) with that of the monosubstituted Schwesinger base (Pyr)P_2-1-Naph (7.07 ppm).[34] Furthermore, the ^{1}H NMR signals for the NHs appeared as triplets due to couplings with both phosphorus atoms which was verified by $^{1}H\{^{31}P\}$ experiments on TPPN and P_2-TPPN samples. The simultaneous coupling of the acidic proton with both phosphorous atoms emphasizes the existence of a low-barrier hydrogen bond. The reaction of TPPN with two equivalents of $HN(SO_2CF_3)_2$ yielded the bisprotonated sponge leading to a further low-field shift in the ^{31}P NMR spectrum ($\delta_{31P}=25.0$ ppm). The acidic protons exhibit a doublet with coupling to only one phosphorus atom ($^{2}J(P,H)=6.5$ Hz) and a chemical shift of 7.65 ppm in the proton NMR spectrum. A similar behavior of the chemical shift is observed in the case of TMGN·HPF_6 ($\delta_{NH}=14.28$ ppm) and the bisprotonated salt $[TMGN\text{-}2H]^{2+}[PF_6]^{-}[BF_4]^{-}$ ($\delta_{NH}=7.84$ ppm).[31a]

Table 1. NMR chemical shifts [ppm] of bisphosphazene proton sponges.

Base	δ_{31P} (free base)	δ_{31P} (protonated form)	$\Delta\delta_{31P}$	δ_{1H} (NH)
TMPN	1.4[a]	29.5[b,d]	28.1	15.84[b]
TBPN	12.8[a]	41.4[b,d]	28.6	15.60[b]
TiPrPN	25.6[b]	54.3[b,e]	28.7	14.05[b]
TcyPPN	21.1[a]	52.8[b,d]	31.7	13.32[b]
HMPN[33]	17.8[b]	33.9[b,d]	16.1	15.0[b]
TPPN[34]	2.5[b]	18.1[b,f]	15.6	15.02[b]
P_2-TPPN[34]	3.2, −3.6[c]	3.7, 1.4[c,f]	–	15.14[b]

[a] in C_6D_6. [b] in $[D_3]$MeCN. [c] in $[D_8]$THF. [d] HPF_6 salt. [e] HBr salt. [f] $HN(SO_2CF_3)_2$ salt.

Structural Features

The structural features of the hydrobromide salt of the four alkyl-substituted bisphosphazene proton sponges, TMPN·HBr (Figure 3),[45] TBPN·HBr (Figure 4),[46] TiPrPN·HBr (Figure 5) and TcyPPN·HBr (Figure 6), were investigated. The nitrogen-bound hydrogen atoms could be located on the Fourier map and were refined isotropically. The molecular structures reveal an unsymmetrical nonlinear hydrogen bridge with the proton preferentially bound to one of the two basic nitrogen atoms. The crystallographic N–H distances range from 0.86(2) Å for TcyPPN·HBr to 0.96(7) Å for TMPN·Br whereas values for *d*(N···H) between 1.77(4) Å for TBPN·HBr and 1.95(7) Å in case of TMPN·HBr were found. Although the accuracy of the bonding and non-bonding N–H distances is intrinsically low, it was observed that the hydrogen bonding is by trend even more unsymmetrical in case of the amino-substituted proton sponges HMPN and P_2-TPPN (*d*(N–H): 0.88(3) Å for HMPN and 0.81(4) Å for P_2-TPPN).[33,34,47] The acidic protons are located in the naphthalene plane showing N-H-N angles of 120(6)° for TMPN·HBr, 146(4)° for TBPN·HBr, 147(4)° for TiPrPN·HBr and 149(2)° for TcyPPN·HBr (the unusual low value observed for TMPN·HBr seems doubtful due to the comparatively low quality of its molecular structure XRD analysis). Furthermore, the acidic protons are located in the naphthalene plane in case of TBPN·HBr, TiPrPN·HBr and TcyPPN·HBr while it stands out of that plane in TMPN·HBr. HMPN·HPF_6 (150(3)°), TPPN·$HN(SO_2CF_3)_2$ (141(2)°) and P_2-TPPN·$HN(SO_2CF_3)_2$ (146(4)°) exhibit similar N–H–N angles to their alkyl-substituted analogs if TMPN·HBr is neglected. The formation of a linear hydrogen bridge is prevented by the short distance between the basicity centers and their lone-pair orientation. An interaction between the acidic proton and the bromide anion is observed in none of the cases. As expected, the double bond between the nitrogen and the phosphorus atom is longer on the side of the protonated nitrogen. The non-bonding distances of the two basicity centers in the protonated alkyl sponges are shorter in case of primary alkyl substituents at the phosphorous atom than for the more bulky isopropyl- and cyclopentyl-substituted deriva-

tives (TMPN·HBr: 2.57(1) Å, TBPN·HBr: 2.594(4) Å, TiPrPN·HBr: 2.634(4) Å, TcyPPN·HBr: 2.641(3) Å). The corresponding values of the amino-substituted analogues range from 2.568(3) Å for HMPN·HPF_6 to 2.600(6) Å for TPPN·$HN(SO_2CF_3)_2$. The remaining literature-known protonated bisphosphazene proton sponges show distances of 2.584(4) and 2.606(4) Å in case of the PPh_3-substituted compound and of 2.534(6) and 2.533(6) Å for the sterically less hindered sponge bearing PPh_2Me moieties.[36b] In theory, protonation leads to a relaxation of the naphthalene backbone. Naphthalene distortion is reflected by the deviation of the average of the torsion angels C1-C8a-C4a-C5 and C8-C8a-C4a-C4 from 180°. The hydrobromides of the alkyl-substituted sponges only show minor distortion which increases with the steric demand of the substituents (TMPN·HBr 1.2(9)°, TBPN·HBr 2.3(3)°, TiPrPN·HBr 3.1(3)°, TcyPPN·HBr 3.7(2)). For TPPN·$HN(SO_2CF_3)_2$ (5.1(4)°) and P_2-TPPN·$HN(SO_2CF_3)_2$ (5.6(3)°) considerably stronger distortions are observed.

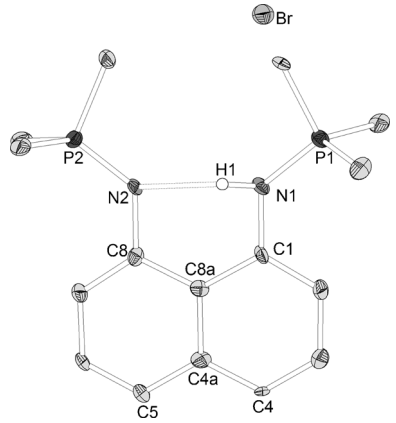

Figure 3. Molecular structure of TMPN·HBr (ellipsoids with 30% probability). Carbon-bonded hydrogen atoms and 1/2 NH_4Br are omitted for clarity. Selected bond lengths [Å] and angles [°]: N1···N11 2.57(1), N1—P1 1.630(8), N2—P2 1.574(7), N1—H1 0.96(7), N2···H1 1.95(7); N1-H1-N2 121(6), C8-C8A-C4A-C4 −179.0(9), C1-C8A-C4A-C5 −178.7(8).[65]

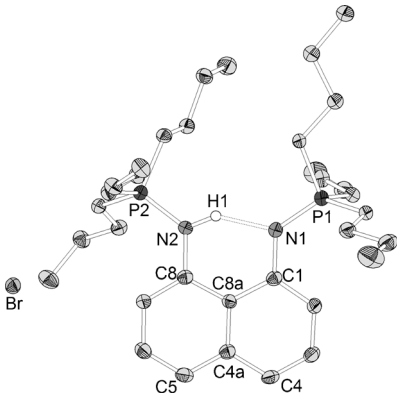

Figure 4. Molecular structure of TBPN·HBr (ellipsoids with 30% probability). Carbon-bonded hydrogen atoms and one THF molecule are omitted for clarity. Selected bond lengths [Å] and angles [°]: N1···N11 2.594(4), N1—P1 1.599(3), N2—P2 1.634(3), N1···H1 1.77(4), N2—H1 0.94(5); N1-H1-N2 146(4), C4-C4A-C8A-C8 178.1(3), C5-C4A-C8A-C1 177.3(3).[65]

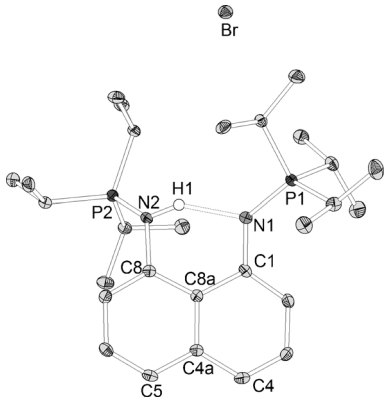

Figure 5. Molecular structure of TiPrPN·HBr (ellipsoids with 30% probability). Carbon-bonded hydrogen atoms are omitted for clarity. Selected bond lengths [Å] and angles [°]: N1···N11 2.634(4), N1—P1 1.602(2), N2—P2 1.647(2), N1···H1 1.81(4), N2—H1 0.93(3); N1-H1-N2 147(4), C4-C4A-C8A-C8 177.4(3), C5-C4A-C8A-C1 176.4(2).[65]

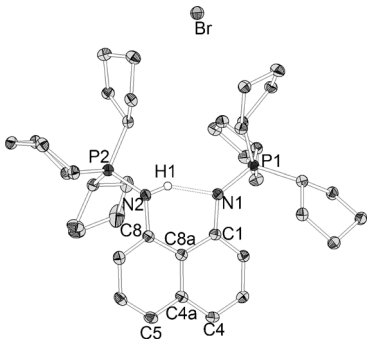

Figure 6. Molecular structure of TcyPPN·HBr (ellipsoids with 30% probability). Carbon-bonded hydrogen atoms are omitted for clarity. Selected bond lengths [Å] and angles [°]: N1···N11 2.641(3), N1—P1 1.600(2), N2—P2 1.648(2), N1···H1 1.87(3), N2—H1 0.86(2); N1-H1-N2 149(2), C4-C4A-C8A-C8 176.4(2), C5-C4A-C8A-C1 176.3(2).

TiPrPN (Figure 7) and TcyPPN (Figure 8) could also be characterized in their initial free base forms. Comparison with the corresponding hydrobromides demonstrates the effect of protonation on the non-bonding N···N distance (reduced from 2.810(2) to 2.634(4) Å in case of TiPrPN and from 2.868(3) to 2.641(3) Å for TcyPPN) and naphthalene distortion (reduced from 7.1(2)° to 3.1(3)° in case of TiPrPN and from 8.1(2)° to 3.7(2)° for TcyPPN). The non-bonding distance of the basic nitrogen atoms in TiPrPN lies between the values observed in HMPN (2.823(2) Å) and the two pyrrolidine-substituted sponges TPPN (2.766(3) Å) and P_2-TPPN (2.763(2) Å). TcyPPN exhibits the longest N···N distance in the studied series (2.868(3) Å). Selected structural features of hydrobromides of the four alkyl-substituted bisphosphazenes' hydrobromides and the free bases TiPrPN and TcyPPN are collected in Table 2.

NMR Titration Experiments

The pK_{BH}^+ values of the four alkyl-substituted bisphosphazene proton sponges were determined by means of NMR titration experiments in acetonitrile. The alkyl sponges competed against HMPN for protons and the equilibrium concentrations

Table 2. Selected structural parameters of bisphosphazene proton sponges in their free base and their protonated forms (bond lengths [Å], angles [°]).

	N···N	N–P	Average naphthalene distortion	N–H	N···H	N–H–N
free bases						
TiPrPN	2.810(2)	1.563(2), 1.562(2)	7.1(2)	–	–	–
TcyPPN	2.868(3)	1.568(2), 1.565(2)	8.1(2)	–	–	–
HMPN[33]	2.823(2)	1.555(1)	6.1(1)	–	–	–
TPPN[34]	2.766(3)	1.550(2), 1.553(2)	8.2(2)	–	–	–
P_2-TPPN[34]	2.763(2)	1.567(2)	6.3(2)	–	–	–
protonated sponges						
TMPN·HBr	2.57(1)	1.630(8), 1.574(7)	1.2(9)	0.96(7)	1.95(7)	120(6)
TBPN·HBr	2.594(4)	1.599(3), 1.634(3)	2.3(3)	0.94(5)	1.77(4)	146(4)
TiPrPN·HBr	2.634(4)	1.602(2), 1.647(2)	3.1(3)	0.93(3)	1.81(4)	147(4)
TcyPPN·HBr	2.641(3)	1.600(2), 1.648(2)	3.7(2)	0.86(2)	1.87(3)	149(2)
HMPN·HPF_6[33]	2.568(3)	1.583(2), 1.604(2)	2.2(2)	0.88(3)	1.76(3)	150(3)
TPPN ·$HN(SO_2CF_3)_2$[34,46]	2.600(6)	1.587(4), 1.597(4)	5.1(4)	0.85(3)	1.88(3)	141(2)
P_2-TPPN ·$HN(SO_2CF_3)_2$[34]	2.570(4)	1.623(3), 1.610(2)	5.6(3)	0.81(4)	1.85(4)	146(4)

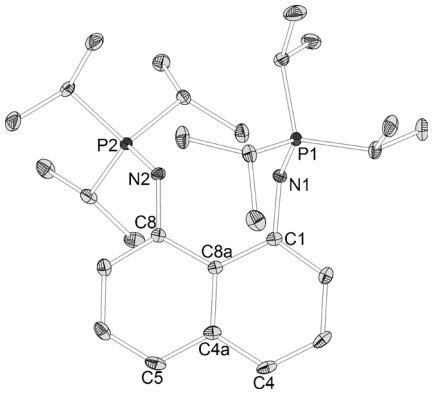

Figure 7. Molecular structure of TiPrPN (ellipsoids with 30% probability). Hydrogen atoms are omitted for clarity. Selected bond lengths [Å] and angles [°]: N1···N11 2.810(2), N1–P1 1.563(2), N2–P2 1.562(2); C1-C8A-4A-C5 172.5(2), C8-C8A-C4A-C4 173.3(2).[65]

were determined by ^{31}P NMR spectroscopy. HMPN turned out to be suitable for these kind of experiments since it exhibits a similar pK_{BH}^+ value of 29.9 in acetonitrile and a very low kinetic basicity resulting in very sharp signals in the ^{31}P NMR spectra. Signals capable of being integrated were also observed for protonated and unprotonated TBPN, TiPrPN and TcyPPN. The kinetically active TMPN and $[TMPN-H]^+$ (see below) showed very broad signals so that only the sharp peaks of HMPN were used for calculation of the equilibrium concentrations of the four species in solution. Hence, we consider the

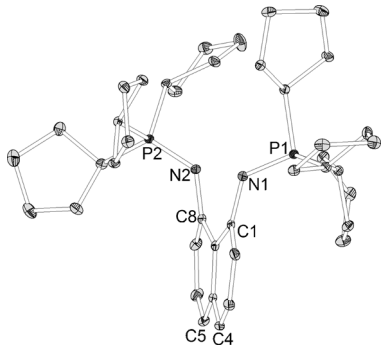

Figure 8. Molecular structure of TcyPPN (ellipsoids with 30% probability). Hydrogen atoms are omitted for clarity. Selected bond lengths [Å] and angles [°]: N1···N11 2.868(3), N1–P1 1.568(2), N2–P2 1.565(2); C5-C4A-C8A-C1 −171.3(2), C4-C4A-C8A-C8 −172.6(2).[65]

value obtained for TMPN to be less accurate since TMPN's free base shows only limited solubility in acetonitrile and even the slightest precipitation of TMPN influences the results. The obtained pK_{BH}^+ values of the alkyl-substituted sponges were cross-checked in NMR-titration experiments among themselves and in case of TBPN and TcyPPN also versus TPPN. The experiments yielded the following pK_{BH}^+ values on the acetonitrile scale: 29.3 for TMPN, 30.4 for TiPrPN, 30.5 for TcyPPN and 30.9 for TBPN. Thus, the basicity of the alkyl-substituted bisphosphazene proton sponges studied herein lies within the same order of magnitude as the basicity of the analogous dimethylamino-substituted HMPN ($pK_{BH}^+(MeCN) = 29.9$).[33] The influence of the different alkyl groups on the pK_{BH}^+ value is discussed in the theoretical section (see below). The pK_{BH}^+ values of naphthalene-based bisphosphazene proton sponges and other chelating hybrid superbases on the acetonitrile scale are presented in Figure 9.

Basic versus Nucleophilic Properties

An important characteristic of a base determining the scope of its synthetic applicability is its nucleophilicity. Since the basic lone pair of a deprotonation reagent can also react with an electrophilic position in the substrate via an S_N2 reaction, undesired side reactions can occur in case of highly nucleophilic bases. A base's nucleophilicity is mainly affected by the steric shielding of the basic site. Hence, a low nucleophilicity could be expected for bisphosphazene proton sponges due to the sterically demanding substituents at the phosphorus atoms. The reaction of a proton sponge with ethyl iodide was chosen as a benchmark to determine the nucleophilic properties in relation to the basic features. When reacting as a base, hydrogen iodide is eliminated to form ethylene in an elimination reaction whereas the ethylated proton sponge is formed from a nucleophilic substitution reaction (Scheme 3). In the latter case the proton sponge loses its rotation symmetry through C4a and C8a and the phosphorus atoms exhibit two signals in the ^{31}P NMR spectrum. Thus, the ratio of protonated to alkylated product can be easily determined by NMR spectroscopy. Furthermore, the alkylated sponge can be detected by ESI mass spectrometry.

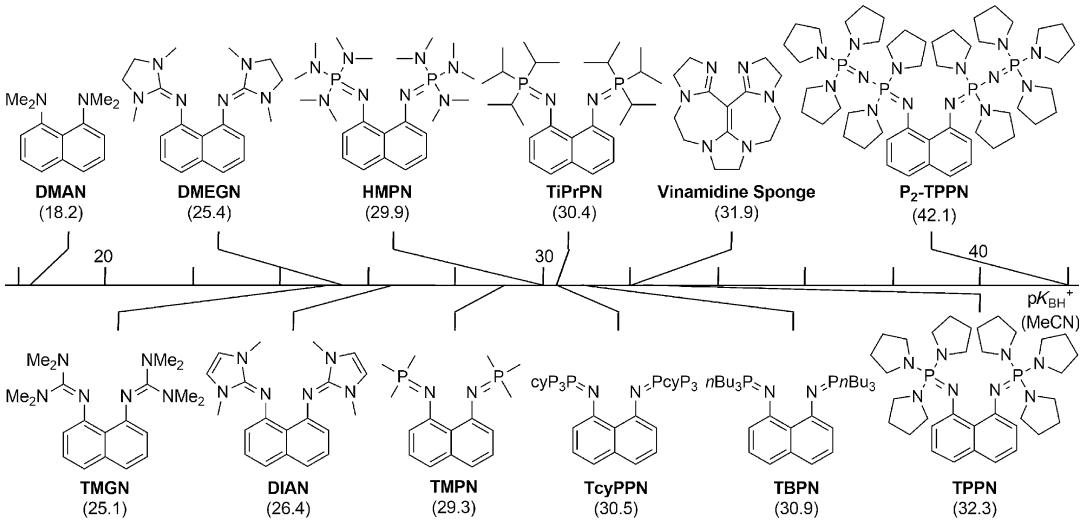

Figure 9. pK_{BH}^{+} values of hybrid proton sponges on the acetonitrile scale.

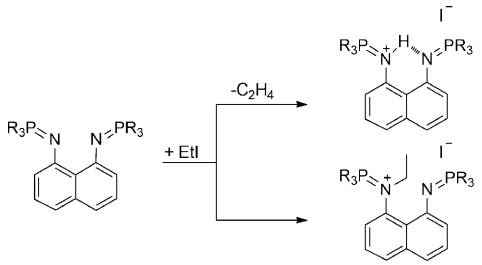

Scheme 3. Reaction of a proton sponge with ethyl iodide.

To our surprise, the alkyl-substituted sponges TMPN, TBPN and TiPrPN exclusively formed the alkylated species from a nucleophilic substitution reaction with ethyl iodide. The remaining alkyl-substituted sponge TcyPPN was reacted with ethyl iodide in THF due to its poor solubility in MeCN. The ^{31}P NMR spectrum of the reaction mixture showed a ratio of 71:29 in favor of the alkylated compound whereas the reaction is slower than observed for the other alkyl-substituted sponges in acetonitrile. A 4:1 ratio in favor of the alkylated species was reported for HMPN in the reaction with ethyl iodide in acetonitrile.[33] The same ratio is found for the related compound TPPN in acetonitrile whereas the ratio is shifted towards the alkylated species when using THF (94:6). The reaction with EtI was carried out in THF for TPPN's higher homologue P_2-TPPN due to its extremely high basicity and it exclusively showed the protonated species which can be referred to the extreme steric shielding of the basicity centers. These findings suggest that some of the applications of the investigated bisphosphazene proton sponges to organic synthesis could be limited by their unexpectedly high nucleophilicity especially in case of the alkyl-substituted compounds. The ratios of alkylation to protonation of the reaction of bisphosphazenes with ethyl iodide are displayed in Table 3 and compared with the nucleophilicity of non-chelating Schwesinger bases that show a lower nucleophilicity and with our bisphosphazene proton pincer P_2-TPPN which is the only superbase in this series revealing a perfect chemoselectivity for the HI elimination reaction. However, a further alkylation experiment showed that P_2-TPPN is readily alkylated by methyl iodide in [D_8]THF at room temperature.

Table 3. Reaction of bisphosphazene proton sponges and non-chelating Schwesinger bases with ethyl iodide.

	Solvent	*T* [°C]	Ratio Alkylation/ protonation	Alkylated species δ (^{31}P NMR) [ppm][a]
TMPN	MeCN	20	100:0	54.6, 13.7
TBPN	MeCN	20	100:0	62.6, 28.6
TiPrPN	MeCN	20	100:0	54.2, 25.5
TcyPPN	THF	20	71:29	66.3, 37.2
HMPN[33]	MeCN	20	80:20	39.1, 29.9
TPPN	MeCN	20	81:19	22.0, 14.0
TPPN	THF	20	94:6	23.4, 14.2
P_2-TPPN	MeCN	20	0:100	–
*t*Oct-$P_2(NMe_2)$[32]	Xylene	70	16:84	–
*t*Bu-$P_1(N(CH_2)_2)$[33]	MeCN	20	40:60	–

[a] The first value can be assigned to the phosphorous atom bound to the alkylated nitrogen atom.

Reactivity towards Group XIII Alkyls

The coordination behavior of DMAN[48] and proton sponges in general towards other electrophiles than protons has only been scarcely investigated. Himmel et al. have studied the coordination chemistry of guanidinyl-substituted proton sponges.[11c,49] Furthermore, palladium, platinum, rhenium, manganese and copper complexes of a sponge related to Staab's quino[7,8*h*]quinoline[20] have been reported.[50] We found that the reaction of TMPN with two equivalents of trimethylaluminum and trimethylgallium in toluene lead to the precipitation of cationic alkyl aluminum or gallium complexes [TMPN-MMe_2]$^+$ with a [MMe_4]$^-$ counteranion (Scheme 4). As observed for the protonation reaction, a low-field shift is found in the ^{31}P NMR spectra with nearly equal values of 38.5 ppm for the aluminum and 38.6 ppm for the gallium species in CD_2Cl_2. A

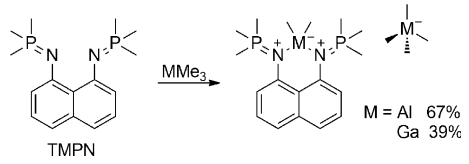

Scheme 4. Conversion of TMPN with group XIII alkyls.

similar reactivity was observed for TPPN yielding $[TPPN\text{-}AlMe_2]^+[AlCl_2Me_2]^-$ after reaction with $Al_2Me_4Cl_2$ (Scheme 5, ^{31}P NMR: $\delta = 26.3$ ppm). Additional experiments to obtain cationic alkyl indium or boron hydride complexes were not successful. Himmel et al. reported a comparable reaction between the tetramethylguanidinyl-substituted proton sponge TMGN with gallium trichloride. Furthermore, they obtained cationic alkylaluminum complexes by the conversion of the protonated sponge with trimethylaluminum under elimination of methane.[49a]

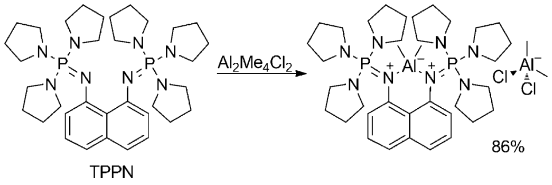

Scheme 5. Reaction of TPPN with $Al_2Me_4Cl_2$.

Recrystallization from dichloromethane/pentane yielded single crystals suitable for X-ray analysis of $[TMPN\text{-}AlMe_2]^+[AlMe_4]^-$ (Figure 10), $[TMPN\text{-}GaMe_2]^+[GaMe_4]^-$ (Figure 11) and $[TPPN\text{-}AlMe_2]^+[AlCl_2Me_2]^-$ (Figure 12). The two structures involving TMPN exhibit equal cell constants revealing a disorder which includes the whole $[TMPN\text{-}MMe_2]^+$ cation. In case of M = Ga only the disordered gallium atom could be located on the Fourier map while the corresponding aluminum compound allowed localization of the disordered Al atom and a fragment of the ligand backbone. The only partly resolved disorders are responsible for the comparably low quality of the structures. Whereas the acidic protons in the examined protonated bisphosphazene sponges are located in the naphthalene plane, the larger aluminum and gallium atoms are displaced outside of this plane. The metal atoms show nearly equal bond lengths to both nitrogen atoms in contrast to the observed unsymmetrical hydrogen bonds in the protonated species. The effect of the coordination of a $[MMe_2]^+$ fragment on the distortion of the naphthalene skeleton is contradictory. Relaxation is observed in case of $[TMPN\text{-}AlMe_2]^+[AlMe_4]^-$ (average distortion: 1.4(5)°), but the molecular structures of $[TMPN\text{-}GaMe_2]^+[GaMe_4]^-$ (5.7(9)°) and $[TPPN\text{-}AlMe_2]^+[AlCl_2Me_2]^-$ (7.8(4)°) still reveal considerable distortion. The structural features of $[TPPN\text{-}AlMe_2]^+[AlCl_2Me_2]^-$ can be compared to those of TPPN's free base form: Interestingly, the aluminum complex exhibits a longer non-bonding distance of the two basic nitrogen atoms than the free base (2.808(8) compared to 2.766(3) Å in TPPN). The large metal alkyl fragments do not fit into the cavity of the proton sponges so that the two nitrogen atoms have to spread away from each other to allow coordination to aluminum or gallium. This is also demonstrated by the unfavorable, nearly rectangular N–M–N angles ($[TPPN\text{-}AlMe_2]^+[AlCl_2Me_2]^-$: 94.1(1)°, $[TMPN\text{-}AlMe_2]^+[AlMe_4]^-$: 91.4(2)°, $[TMPN\text{-}GaMe_2]^+[GaMe_4]^-$: 87.4(3)°). Selected structural features of the three metal complexes are collected in Table 4.

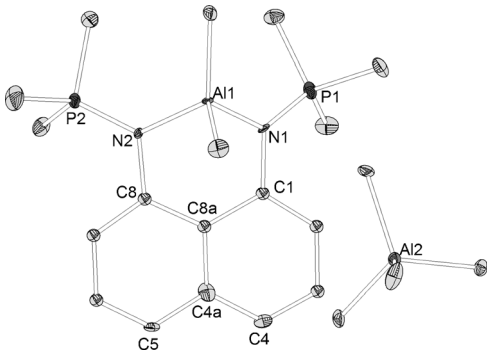

Figure 10. Molecular structure of $[TMPN\text{-}AlMe_2]^+[AlMe_4]^-$ (ellipsoids with 30% probability). Hydrogen atoms are omitted for clarity. Selected bond lengths [Å] and angles [°]: N1···N11 2.749(6), N1—P1 1.588(5), N2—P2 1.599(5), N1—Al1 1.917(5), N2—Al1 1.925(5); N1-Al1-N2 91.4(2), C5-C4A-C8A-C1 −177.8(5), C4-C4A-C8A-C8 179.4(5).[65]

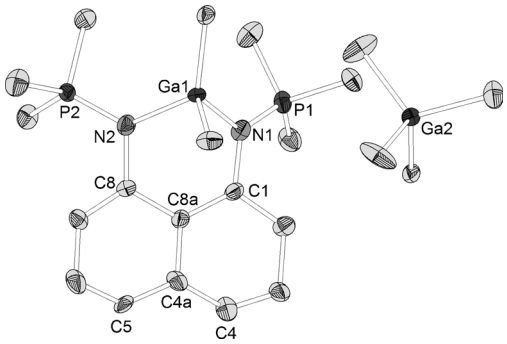

Figure 11. Molecular structure of $[TMPN\text{-}GaMe_2]^+[GaMe_4]^-$ (ellipsoids with 30% probability). Hydrogen atoms are omitted for clarity. Selected bond lengths [Å] and angles [°]: N1···N11 2.74(1), N1—P1 1.551(8), N2—P2 1.602(7), N1—Ga1 1.990(7), N2—Ga1 1.979(7); N1-Ga1-N2 87.4(3), C5-C4A-C8A-C1 −172.7(9), C4-C4A-C8A-C8: 175.9(9).[65]

Table 4. Selected structural parameters of cationic Group XIII metal complexes of bisphosphazene proton sponges (bond lengths [Å], angles [°]).

	N···N	N–P	Average naphthalene distortion	N–M	N–M–N
$[TMPN\text{-}AlMe_2]^+[AlMe_4]^-$	2.749(6)	1.588(5), 1.599(5)	1.4(5)	1.917(5), 1.925(5)	91.4(2)
$[TMPN\text{-}GaMe_2]^+[GaMe_4]^-$	2.74(1)	1.551(8), 1.602(7)	5.7(9)	1.990(7), 1.979(7)	87.4(3)
$[TPPN\text{-}AlMe_2]^+[AlMe_2Cl_2]^-$	2.808(8)	1.624(3), 1.636(3)	7.8(4)	1.897(3), 1.939(4)	94.1(1)

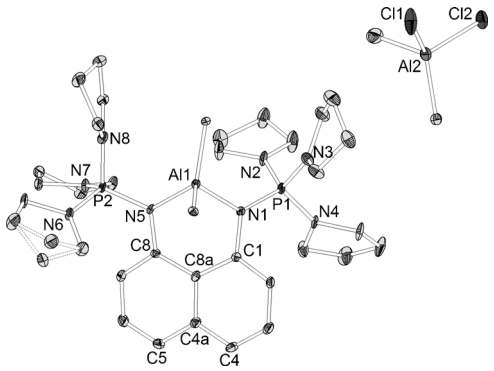

Figure 12. Molecular structure of $[TPPN\text{-}AlMe_2]^+[AlCl_2Me_2]^-$ (ellipsoids with 30% probability). Hydrogen atoms are omitted for clarity. A disorder observed for the anion is not displayed. Selected bond lengths [Å] and angles [°]: N1···N11 2.808(8), N1—P1 1.624(3), N5—P2 1.636(3), N1—Al1 1.897(3), N5—Al1 1.939(4); N1-Al1-N5 94.11(14), C5-C4A-C8A-C1 −172.4(3), C4-C4A-C8A-C8 −172.1(4).[65]

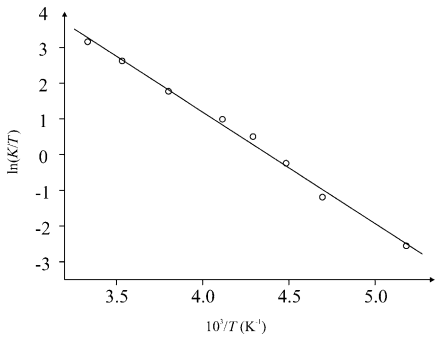

Figure 13. Eyring plot of the methyl groups of TMPN with $TMPNH^+$ (0.45:0.55) in $[D_8]$THF.

Kinetic Basicity

The kinetic basicity is expressed by the proton self-exchange rate and is usually very low for proton sponges due to the steric shielding of the acidic proton by bulky hydrophobic substituents (see above). We exemplarily investigated the kinetic basicity of the two bisphosphazene proton sponges TMPN and TPPN and determined self-exchange rates k as well as the corresponding free activation energies $\Delta G^{\neq}$ at different temperatures. Generally, a solution of the proton sponge's free base form in $[D_8]$THF was combined with a solution of the protonated sponge in the same solvent. Preliminary experiments indicated that the proton self-exchange processes for TMPN and TPPN take place on different time scales and thus different NMR spectroscopic techniques are required for the investigation of kinetic processes.

Line-shape analysis is usually used to quantitatively study exchange processes when the spectra of all three regions of the exchange processes, these are, slow exchange, intermediate (where the coalescence point sits) and fast exchange, are obtainable. The comparably high kinetic activity of TMPN allowed the application of this technique using a Bruker DRX 500 spectrometer at temperatures ranging from 193 to 300 K. In the following only the dynamic behavior of the ^{1}H NMR signals of the methyl groups will be discussed. Only one signal is observed for the two species' methyl groups at 300 K. The decrease in temperature results in the broadening of the signal until coalescence is reached at 243 K. At 193 K two separated sharp doublets were observed at 2.006 ppm (^3J(P,H) = 14 Hz) and 1.565 ppm (^3J(P,H) = 13 Hz) for the methyl groups of $TMPN{\cdot}H^+$ and TMPN, respectively. At a resonance frequency of 500 MHz, this corresponds to a frequency difference of 220 Hz between the two exchanging sites. Furthermore, from the signal intensities at 193 K a molar ratio of 0.45:0.55 was determined for $TMPN/TMPN{\cdot}H^+$ in the sample used.

Line-shape analysis of the variable temperature ^{1}H NMR spectra was done using the program DNMR within the Bruker program package Topspin 3.2 (Figure S1.1). Results of the line-shape analysis are a set of the exchange rates k and simulated spectra. By linear fitting of ln(k/T) versus (1/T) via an Eyring plot one obtains the free energy, enthalpy and entropy of activation (Figure 13).

The results of the quantitative dynamic study on the proton self-exchange between TMPN and $TMPN{\cdot}H^+$ in THF on the ^{1}H NMR signals of the methyl groups are summarized in Table 5. Furthermore, a corresponding activation enthalpy of 26.6 kJ mol^{-1} and an activation entropy of −83.8 J mol^{-1} K^{-1} were determined. The detailed procedure is explained in the Supporting Information.

Table 5. Proton self-exchange of TMPN and $TMPN{\cdot}HN(SO_2CF_3)_2$ in $[D_8]$THF.

T [K]	Exchange rate k [s^{-1}]	Free energy $\Delta G^{\neq}$ [kJ mol^{-1}]
193	13	42
213	64	44
223	173	45
233	385	45
243	660	46
263	1545	48
283	3890	50
300	7050	51

The considerably lower kinetic basicity of TPPN did not allow the application of line shape analysis since the corresponding coalescence temperature lies far above the boiling point of THF. Therefore, exchange spectroscopy (EXSY) was used which is appropriate for the study of slow chemical exchange whereby no coalescence can be observed.[51]

The ^{31}P,^{31}P EXSY experiments were run on a mixture of TPPN and $TPPN{\cdot}HN(SO_2CF_3)_2$ in $[D_8]$THF using a standard pulse sequence at a Bruker AV III 500 spectrometer.[52] The spectral width for the 2D EXSY was 40 ppm with a relaxation delay of 15 s. The mixing time was 50 ms at 300 K and 10 ms at 323 and 333 K. Since the experiment is extremely time-consuming, the kinetic basicity of TPPN was studied at only three different temperatures. A free activation energy for proton self-exchange of 66 kJ mol^{-1} was observed at 300 K. The activation enthalpy is 35 kJ mol^{-1} and an activation entropy of −102 J mol^{-1} K was determined. The EXSY results for the TPPN and $TPPN{\cdot}H^+$ self-exchange in $[D_8]$THF are summarized in

Table S1.12 and the corresponding Eyring plot is shown in Figure S1.2. The detailed procedure is explained in the Supporting Information.

Up to now, the only free activation energy for proton self-exchange determined for proton sponges has been 59.3 kJ mol^{-1} for TMGN with a coalescence temperature at 300 K for ^{1}H NMR spectra observed in [D$_3$]MeCN on a 500 MHz resonance frequency. The corresponding value for DMAN was estimated to be more than 66 kJ mol^{-1} in [D$_3$]MeCN because the coalescence temperature was above the boiling point of the solvent.[33a] Thus, $\Delta G^{\neq}$ for TPPN lies between the values of TMGN and DMAN. The comparatively little steric shielding of the basicity centers by TMPN's methyl groups results in a comparably low free activation energy of 51 kJ mol^{-1} for this bisphosphazene sponge. Thus, TMPN is a kinetically active representative of the compound class of proton sponges.

Theoretical Section

The gas-phase proton affinities (PA) and gas-phase basicities (GB) of the proton sponges TMPN, TiPrPN, TBPN and TcyPPN, together with their monosubstituted analogues, are calculated at B3LYP/6-311 + G(2df,p)//B3LYP/6-31G(d) level, taking into account the thermal corrections estimated by the B3LYP/6-31G(d) method. They are presented in Table 6. All calculations were done utilizing the Gaussian03 program package.[53] The proton affinities of the alkyl-substituted bisphosphazene proton sponges range from 271.8 kcal mol^{-1} (1137.2 kJ mol^{-1}) (TMPN) to 279.0 kcal mol^{-1} (1167.3 kJ mol^{-1}) (TcypPN), thus being slightly lower/higher than the PA of Schwesinger's *t*Bu-P$_2$ phosphazene (PA = 274.4 kcal mol^{-1} (1148.1 kJ mol^{-1})).[54] Generally, there are two main contributions that determine the proton affinities of the proton sponges: 1) the intrinsic basicity of the basic fragments that undergo protonation and 2) the proton chelating effect.[34] The contribution to the PA due to the chelating effect is a consequence of: a) the destabilization in the neutral base induced mainly by a strong repulsion of unshared electron pairs that diminishes after protonation and b) the formation of an intramolecular hydrogen bond (IMHB) in the protonated form. The chelating effect can be expressed as a difference in the PA of the monosubstituted analogue of the proton sponge and the proton sponge itself. For TMPN, TiPrPN, TBPN and TcyPPN, the chelating effect contributes to the PA by 25.8 (107.9), 24.7 (103.3), 26.7 (111.7) and 26.1 kcal mol^{-1} (109.2 kJ mol^{-1}), respectively. Interestingly, this contribution is very similar for all four proton sponges, the biggest difference being 2.0 kcal mol^{-1} (8.4 kJ mol^{-1}). This is an interesting finding since it would be expected that, due to a higher strain in the neutral base, the bulkier P(cyP)$_3$ substituent would lead to a higher value for the chelating effect in TcyPPN than the relatively small PMe$_3$ substituent should do in TMPN. To quantify the influence of the destabilization energy (E_d) in the neutral base and the stabilization energy (E_s) in the conjugate acid, homodesmotic reactions were used analogously to the procedure applied in our previous papers.[33,34] It appears that the destabilization energy is indeed the largest in TcyPPN, being 13.8 (57.7), 14.7 (61.5), 14.3 (59.8) and 18.7 kcal mol^{-1} (78.2 kJ mol^{-1}) for TMPN, TiPrPN, TBPN and TcyPPN, respectively. However, the stabilization energy in the conjugated acid is 11.9 (49.8), 10.3 (43.1), 12.4 (51.9) and 7.4 kcal mol^{-1} (31.0 kJ mol^{-1}), correspondingly. Since the chelating effect is the sum of E_d and E_s, it appears that the much higher E_d in TcyPPN is partially compensated by a lower E_s value. The main contribution to the E_s energy in conjugated acids of proton sponges is the stabilization due to the formation of the intramolecular hydrogen bond. Since it is not likely that the hydrogen bond in TcyPPN is much weaker than in the other three sponges, the lower stabilization energy could be explained only by 'lingering' strain (a part of the strain still exists in the conjugated acid).[55]

Table 6. Theoretically obtained gas phase proton affinities (PA) and gas-phase basicities (GB) in [kcal mol^{-1}] and [kJ mol^{-1}] (in parentheses) together with pK_{BH^+} values in acetonitrile of bisphosphazene proton sponges, their monophosphazene analogues and the corresponding basic fragments.

Base	PA	GB	pK_{BH^+}(MeCN)
TMPN	271.8 (1137.2)	262.7 (1099.1)	29.7
TiPrPN	275.1 (1151.0)	267.9 (1120.9)	30.9
TBPN	278.8 (1166.5)	269.5 (1127.6)	30.0
TcypPN	279.0 (1167.3)	271.1 (1134.3)	32.2
Me$_3$P=NNaph	246.0 (1029.3)	238.5 (997.9)	19.2
*i*Pr$_3$P=NNaph	250.4 (1047.7)	242.6 (1015.0)	19.1
*n*Bu$_3$P=NNaph	252.1 (1054.8)	243.9 (1020.5)	19.1
(cyP)$_3$P=NNaph	252.9 (1058.1)	244.4 (1022.6)	19.1
Me$_3$P=NH	249.4 (1043.5)	242.1 (1012.9)	25.6
*i*Pr$_3$P=NH	254.5 (1064.8)	247.5 (1035.5)	24.5
*n*Bu$_3$P=NH	257.4 (1077.0)	250.6 (1048.5)	24.8
(cyP)$_3$P=NH	259.9 (1087.4)	252.4 (1056.0)	25.6

Since the spread between the PA of the lowest basic proton sponge TMPN and the most basic one TcyPPN is 7.2 kcal mol^{-1} (30.1 kJ mol^{-1}), and the energy of chelating effect for all four sponges is very similar, the main contribution to the difference in PA should then be the difference in proton affinity of the basic fragments. The perusal of the PA for fragments R$_3$P=NNaph reveals that the PA increases along the series in a similar manner to the four proton sponges. The increase in PA of the basic fragments when going from methyl to cyclopentyl can be attributed to an increase in the electron donor ability of the larger alkyl groups attached to the phosphorus atom.

Therefore, it may be concluded that the increase in the PA values of proton sponges when going from TMPN to TcyPPN is a consequence of the higher basicity of the basic substituents whereas the chelating effect plays a minor role.

Let us compare now the basicities of TcyPPN and the recently synthesized TPPN (PA = 283.2 kcal mol^{-1} (1194.9 kJ mol^{-1})).[34] TcypPN has a lower PA than TPPN by 4.2 kcal mol^{-1} (17.6 kJ mol^{-1}). In the former, cyclopentyl groups are attached to a phosphorus atom, whereas the latter possess pyrrolidinyl groups instead. Both substituents have approximately the same steric demand which results in exactly the same chelating energy of 26.1 kcal mol^{-1} (109.2 kJ mol^{-1}). However, the PA of the ((CH$_2$)$_4$N)$_3$P=NH is by 3.2 kcal mol^{-1} (13.4 kJ mol^{-1}) higher than the PA of the (cyP)$_3$P=NH as a result of a stronger electron

donating ability of the dialkylamino group. Like among the alkyl-substituted bisphosphazenes, the main reason for a difference in basicities of TcyPPN and TPPN is a difference in the basicity of their basic fragments.

Theoretical calculations of the pK_{BH}^{+} values in acetonitrile were performed using the isodensity polarized continuum model (IPCM); the detailed procedure is described elsewhere.[54] The pK_{BH}^{+} values for the alkyl-substituted bisphosphazene proton sponges, together with their monosubstituted analogues, are presented in Table 6. Most of them are in reasonable agreement with the experimental data–discrepancies are smaller than 1 unit for TMPN, TiPrPN and TBPN. However, the theoretical value for TcyPPN is by 1.7 units higher than the experimental one. The estimated average absolute error for the applied theoretical model is ± 0.4 units for phosphazene superbases.[54] The discrepancy of 1.7 units is far beyond that value. However, the experimental pK_{BH}^{+} value of TcyPPN is very similar to the pK_{BH}^{+} value of TBPN. Since both sponges have a very similar gas phase PA, the experimental pK_{BH}^{+} seems to be more realistic. The error in the theoretical pK_{BH}^{+} probably arises from the inaccuracy in the solvation energy calculation or from the approximation that the most stable conformer in the gas phase is at the same time the most stable conformer in solution (conformational analysis is not performed in solution).

Conclusion and Outlook

The class of superbasic bisphosphazene proton sponges was extended by four alkyl-substituted representatives that populate the scale of pK_{BH}^{+} values in acetonitrile in the region around 30. The dramatic effect of proton chelation on the basicity was rationalized by means of X-ray crystallographic data and computational studies underlining the great potential of combining superbasicity concepts for the design of new powerful nonionic bases. Not only their remarkable basic properties but also their easy and upscalable synthesis routes via a Kirsanov reaction as the key step could make the alkyl-substituted bisphosphazenes interesting organocatalysts in base-mediated reactions. Future experiments will have to show if their high nucleophilicity limits their applicability in organic synthesis. Furthermore, NMR spectroscopic studies on the kinetic basicity of TMPN and TPPN gave valuable information about their potential to act as bases in catalytic processes and in the future we would like to use the established methods for the determination of the kinetic activity to other superbases. Eventually, we provided first insight into the coordination behavior of TMPN and TPPN and thereby presented rare examples of metal complexes of proton sponges. We expect that such chelating superbases will exhibit a rich coordination chemistry as superdonors towards highly electrophilic and coordinatively unsaturated metal centers.

Experimental Section

All reactions were carried out under inert atmosphere using standard Schlenk techniques. Moisture and air sensitive substances were stored in a conventional nitrogen-flushed glovebox. Solvents were purified according to literature procedures and kept under an inert atmosphere. Trimethylphosphane[56] and triisopropylphosphane[57] were prepared according to literature-known procedures. Tricyclopentylphosphane and tributylphosphane were acquired by purchase whereas the latter was purified by condensation prior to use. 1,8-Diaminonaphthalene (Acros) was purified by recrystallization from toluene followed by sublimation. Tris(pyrrolidinyl)phosphane was prepared via a condensation reaction from PCl_3.[58] The oxidation of phosphanes by bromine was performed on the basis of literature-known protocols in benzene.[59] $NaN(SiMe_3)_2$[60] and $KN(SiMe_3)_2$[61] were prepared by deprotonation of $HN(SiMe_3)_2$ by $NaNH_2$ or KH, respectively.

Spectra were recorded on the following spectrometers: NMR: ^1H and ^{31}P spectra were recorded on a Bruker AVANCE 300 spectrometer installed with an automatic sample changer; standard ^1H–^1H and ^1H–^{13}C 2D spectra, the ^{31}P decoupled spectra $^1H\{^{31}P\}$, and $^{13}C\{^{31}P\}$, as well as low temperature ^1H spectra were recorded on a Bruker DRX 500 spectrometer installed with an inverse triple-resonance probe; ^{31}P–^{31}P EXSY spectra at variable temperatures were taken on a Bruker AVANCE 500 spectrometer with a BBFO probe. Mixing times of 10 and 50 ms were used, and spectra were collected with 4096 points in the F_2 dimension, 128 increments in the F_1 dimension, 16 transients for each increment, and a relaxation delay of 15 s. Typical experiment time was about 9 h per spectrum; IR: ATR-FT-IR; MS: LTQ-FT or QStarPulsar i (Finnigan); elemental analysis: CHN-Rapid (Heraeus).

1,8-Bis(tributylphosphazenyl)naphthalene (TBPN): Bromine (3.90 g, 24.40 mmol, 2.0 equiv) was added dropwise to a solution of tributylphosphane (4.94 g, 24.40 mmol, 2.0 equiv) in chlorobenzene (200 mL) at 0 °C. A yellow solid precipitated and the suspension was stirred for 1.5 h at 0 °C and additional 1.5 h at room temperature. A solution of 1,8-diaminonaphthalene (1.93 g, 12.19 mmol, 1.0 equiv) and triethylamine (4.94 g, 48.79 mmol, 4.0 equiv) in chlorobenzene (25 mL) was added dropwise at 0 °C and the reaction mixture was stirred for 2 h at room temperature and additional 16 h at 80 °C. The hot suspension was filtered over celite and a solution of $KN(SiMe_3)_2$ (2.43 g, 12.19 mmol, 1.0 equiv) in toluene (30 mL) was added dropwise at 0 °C. The reaction mixture was stirred overnight and separated from precipitated KBr via filtration over celite. The filtrate was evaporated to dryness in vacuo and pentane (100 mL) was added to the oily residue. The suspension was filtered over celite and the solvent was removed in vacuo from the filtrate to yield TBPN (6.10 g, 93%). The spectroscopic and analytic data are in accord with the literature ^1H NMR (300 MHz, [D_6]benzene, 25 °C, TMS): $\delta = 7.42$ (dt, $^3J(H,H) = 8.0$ Hz, $^4J(H,H) = 1.8$ Hz, 2H, H(4,5)), 7.33 (t, $^3J(H,H) = 7.6$ Hz, 2H, H(3,6)), 6.80–6.76 (m, 2H, H(2,7)), 1.73–1.63 (m, 12H, H(9)), 1.50–1.38 (m, 12H, H(10)), 1.24 (sext, $^3J(H,H) = 7.2$ Hz, 12H, H(11)), 0.82 ppm (t, $^3J(H,H) = 7.3$ Hz, 18H, H(12)); ^{13}C NMR (76 MHz, [D_6]benzene, 25 °C, TMS): $\delta = 153.0$ (C(1,8)), 139.3 (C(4a)), 131.3 (t, $^3J(P,C) = 12.1$ Hz, C(8a)), 125.4 (C(3,6)), 119.0 (d, $^3J(P,C) = 11.7$ Hz, C(2,7)), 118.5 (C(4,5)), 27.0 (d, $^1J(P,C) = 62.8$ Hz, C(9)), 24.9 (C(10)), 24.8 (d, $^3J(P,C) = 8.9$ Hz, C(11)), 13.9 ppm (C(12)); ^{31}P NMR (101.3 MHz, [D_6]benzene, 25 °C, 85% H_3PO_4): $\delta = 12.8$ ppm; IR: $\tilde{\nu} = 485, 549, 636, 719, 746, 777, 815, 899, 936, 967, 1002, 1053, 1091, 1122, 1184, 1208, 1285, 1336, 1376, 1428, 1500, 1544, 1590, 2869, 2928, 2955, 3040$ cm^{-1}; ESI-MS (MeCN): *m/z* (%): 560 (100) $[M]^+$; HRMS (ESI): *m/z* calcd for $C_{34}H_{61}N_2P_2^+$: 559.4310 $[M+H^+]$; found: 559.4290.

TBPN·HPF$_6$: A solution of NH_4PF_6 (0.384 g, 2.355 mmol, 1.0 equiv) in THF (20 mL) was added dropwise to a solution of TBPN (1.316 g, 2.355 mmol, 1.0 equiv) in THF (20 mL) at 0 °C. After stirring the reaction mixture for 2 h at room temperature, all volatiles were re-

moved in vacuo and the oily residue was triturated three times with diethyl ether (20 mL). TBPN·HPF_6 (1.170 g, 70%) was obtained as a beige solid.[62] ^{1}H NMR (300 MHz, [D_3]MeCN, 25 °C, TMS): δ = 15.64 (t, ^3J(P,H) = 3.3 Hz, 1H, NH), 7.22–7.15 (m, 4H, H(3,4,5,6)), 6.63–6.60 (m, 2H, H(2,7)), 2.25–2.16 (m, 12H, H(9)), 1.57–1.36 (m, 24H, H(10,11)), 0.88 ppm (t, ^3J(H,H) = 7.1 Hz, 18H, H(12)); ^{13}C NMR (100.6 MHz, [D_3]MeCN, 25 °C, TMS): δ = 145.8 (d, ^2J(P,C) = 2.8 Hz, C(1,8)), 138.1 (C(4a)), 127.2 (C(4,5)), 120.7 (t, ^3J(P,C) = 11.1 Hz, C(8a)), 120.6 (C(3,6)), 113.0 (d, ^3J(P,C) = 8.7 Hz, C(2,7)), 24.3 (d, ^3J(P,C) = 15.4 Hz, C(11)), 24.0 (d, ^2J(P,C) = 3.5 Hz, C(10)), 23.0 (d, ^1J(P,C) = 60.0 Hz, C(9)), 13.7 ppm (C(12)); ^{31}P NMR (121.5 MHz, [D_3]MeCN, 25 °C, 85% H_3PO_4): δ = 41.4 (s, -PBu_3), −145.4 ppm (sept, ^1J(P,F) = 706.3 Hz, PF_6^-); IR: $\tilde{\nu}$ = 417, 486, 556, 640, 714, 757, 833, 876, 908, 930, 970, 1052, 1079, 1127, 1185, 1234, 1290, 1333, 1381, 1455, 1509, 1572, 2871, 2931, 2957 cm^{-1}; ESI-MS (MeCN): *m/z* (%): 560 (100) $[M]^+$, 359 (4) $[C_{22}H_{36}N_2P]^+$; HRMS (ESI): *m/z* calcd for $C_{34}H_{61}N_2P_2^+$: 559.4304 $[M]^+$; found: 559.4296; (−)-ESI-MS (MeCN): *m/z* (%): 145 (100) $[PF_6]^-$; HRMS ((−)-ESI): *m/z* calcd for PF_6^-: 144.9647 $[M]^-$; found: 144.9648; elemental analysis calcd (%) for $C_{34}H_{61}F_6N_2P_3$: C 57.94, H 8.72, N 3.97; found: C 57.58, H 8.97, N 4.04.

1,8-Bis(trimethylphosphazenyl)naphthalene (TMPN): Bromine (3.09 g, 19.32 mmol, 2.1 equiv) was added slowly to a solution of trimethylphosphane (1.47 g, 19.32 mmol, 2.1 equiv) in benzene (100 mL) at 0 °C. An orange solid precipitated and the suspension was stirred for 30 min at 0 °C and additional 2 h at room temperature. A solution of 1,8-diaminonaphthalene (1.45 g, 9.20 mmol, 1.0 equiv) and triethylamine (3.90 g, 38.64 mmol, 4.2 equiv) in toluene (20 mL) was added dropwise and the black reaction mixture was stirred for 1 h at room temperature and additional 16 h at 70 °C. The suspension was cooled to room temperature and a solution of $KN(SiMe_3)_2$ (7.34 g, 36.80 mmol, 4.0 equiv) in toluene (40 mL) was added dropwise. The reaction mixture was stirred for 2 h at room temperature and precipitated potassium bromide was separated by filtration over celite. The solid was extracted twice with toluene (20 mL). The toluene phases were combined with the filtrate and evaporated to dryness in vacuo. The residue was suspended in hexane (40 mL) and the solid was separated by filtration, washed twice with hexane (20 mL) and dried in vacuo. TMPN (1.87 g, 67%) was obtained as a dark brown solid. ^{1}H NMR (400 MHz, [D_3]MeCN, 25 °C, TMS): δ = 6.97 (t, ^3J(H,H) = 7.6 Hz, 2H, H(3,6)), 6.92 (dt, ^3J(H,H) = 8.0 Hz, ^4J(H,H) = 1.6 Hz, 2H, H(4,5)), 6.34 (ddd, ^3J(H,H) = 7.1 Hz, J = 3.2 Hz,[63] ^4J(H,H) = 1.5 Hz, 2H, H(2,7)), 1.52 ppm (d, ^2J(P,H) = 12.5 Hz, 18H, H(9)); ^{13}C NMR (101 MHz, [D_3]MeCN, 25 °C, TMS): δ = 153.0 (d, ^2J(P,C) = 3.5 Hz, C(1,8)), 139.9 (C(4a)), 129.9 (t, ^3J(P,C) = 7.8 Hz, C(8a)), 126.2 (C(3,6)), 118.0 (d, ^3J(P,C) = 14.6 Hz, C(2,7)), 117.8 (C(4,5)), 16.7 ppm (d, ^1J(P,C) = 69.9 Hz, C(9)); ^{31}P NMR (101 MHz, [D_6]benzene, 25 °C, 85% H_3PO_4): δ = 1.4 ppm; IR: $\tilde{\nu}$ = 480, 510, 551, 640, 665, 720, 742, 775, 813, 832, 852, 917, 931, 979, 1003, 1054, 1119, 1186, 1281, 1344, 1380, 1429, 1500, 1538, 2906, 2974, 3034 cm^{-1}; ESI-MS (MeCN): *m/z* (%): 307(40) $[M]^+$, 233 (100) $[M-PMe_3]^+$; HRMS (ESI): *m/z* calcd for $C_{16}H_{25}N_2P_2^+$: 307.1493 $[M]^+$; found: 307.1487; elemental analysis calcd (%) for $C_{16}H_{24}N_2P_2$: C 62.73, H 7.90, N 9.15; found: C 61.96, H 7.90, N 9.21.

TMPN·HPF_6: A solution of NH_4PF_6 (160 mg, 0.979 mmol, 1.0 equiv) in THF (10 mL) was added dropwise to a solution of TMPN (300 mg, 0.979 mmol, 1.0 equiv) in THF (20 mL). A white solid precipitated and the suspension was stirred for 1 h at room temperature. The reaction mixture was concentrated in vacuo to about 10 mL and the precipitate was collected by filtration. The solid was washed twice with diethyl ether (20 mL) and dried in vacuo. TMPN·HPF_6 (275 mg, 62%) was obtained as a white solid. ^{1}H NMR (300 MHz, [D_3]MeCN, 25 °C, TMS): δ = 15.84 (br s, 1H, NH), 7.20–7.19 (m, 4H, H(3,4,5,6)), 6.58–6.55 (m, 2H, H(2,7)), 1.93 ppm (d, ^2J(P,H) = 13.5 Hz, 18H, H(9)); ^{13}C NMR (126 MHz, [D_3]MeCN, 25 °C, TMS): δ = 145.7 (C(1,8)), 138.3 (C(4a)), 127.2 (C(4,5)), 120.4 (t, ^3J(P,C) = 12.1 Hz, C(8a)), 120.3 (C(3,6)), 112.3 (d, ^3J(P,C) = 10.7 Hz, C(2,7)), 13.5 ppm (d, ^1J(P,C) = 66.9 Hz, C(9)); ^{31}P NMR (122 MHz, [D_3]MeCN, 25 °C, 85% H_3PO_4): δ = 29.5 (s, -PMe_3), −145.5 ppm (sept, ^1J(P,F) = 706.3 Hz, PF_6^-); IR: $\tilde{\nu}$ = 486, 555, 632, 664, 685, 762, 820, 876, 960, 1051, 1083, 1133, 1294, 1326, 1409, 1458, 1512, 1573, 1609, 2871, 2931, 2958 cm^{-1}; ESI-MS (MeCN): *m/z* (%): 307 (100) $[M]^+$; HRMS (ESI): *m/z* calcd for $C_{16}H_{25}N_2P_2^+$: 307.1487 $[M]^+$; found: 307.1482; (−)-ESI-MS (MeCN): *m/z* (%): 145 (100) $[PF_6]^-$; HRMS ((−)-ESI): *m/z* calcd for PF_6^-: 144.9647 $[M]^-$; found: 144.9646; elemental analysis calcd (%) for $C_{16}H_{25}F_6N_2P_3$: C 42.29, H 5.57, N 6.19; found: C 42.11, H 5.55, N 6.41.

1,8-Bis(triisopropylphosphazenyl)naphthalene hydrobromide (TiPrPN·HBr): A solution of 1,8-diaminonaphthalene (297 mg, 1.87 mmol, 1.0 equiv) and triethylamine (759 mg, 7.50 mmol, 4.0 eq) in chlorobenzene (20 mL) was added dropwise to a suspension of triisopropylbromophosphoniumbromide (1200 mg, 3.75 mmol, 2.0 equiv) in chlorobenzene (40 mL). The grey reaction mixture changed color to light brown and was stirred for 1 h at 90 °C. A solution of $NaN(SiMe_3)_2$ (1031 mg, 5.63 mmol, 3.0 equiv) in chlorobenzene (20 mL) was added at room temperature and the reaction mixture was stirred for 2 h at 90 °C. The hot solution was filtered over celite and the filtrate was evaporated to dryness in vacuo. The oily residue was washed with hexane to give a powdery raw product which was washed with THF. The remaining solid was dried in vacuo to give TiPrPN·HBr (780 mg, 1.40 mmol, 75%) as a beige solid. Single crystals suitable for structure determination were obtained by layering a saturated solution of TiPrPN·HBr in acetonitrile with diethyl ether. ^{1}H NMR (300 MHz, [D_3]MeCN, 25 °C, TMS): δ = 14.05 (br s,s 1H, NH), 7.30 (d, ^3J(H,H) = 8.2 Hz, 2H, H(4,5)), 7.21 (t, ^3J(H,H) = 7.8 Hz, 2H, H(3,6)), 6.78 (d, ^3J(H,H) = 7.4 Hz, 2H, H(2,7)), 2.84 (dsept, ^3J(H,H) = 7.3 Hz, ^2J(P,H) = 12.0 Hz, 6H, H(9)), 1.30 ppm (dd, ^3J(H,H) = 7.3 Hz, ^3J(P,H) = 15.6 Hz, 36H, H(10)); ^{13}C NMR (126 MHz, [D_3]MeCN, 25 °C, TMS): δ = 145.3 (d, ^2J(P,C) = 4.0 Hz, C(1,8)), 137.7 (C(4a)), 127.0 (C(4,5)), 123.4 (t, ^3J(P,C) = 9.1 Hz, C(8a)), 121.5 (C(3,6)), 116.1 (d, ^3J(P,C) = 4.8 Hz, C(2,7)), 25.5 (d, ^1J(P,C) = 54.4 Hz, C(9)), 17.1 ppm (d, ^2J(P,C) = 2.5 Hz, C(10)); ^{31}P NMR (122 MHz, [D_3]MeCN, 25 °C, 85% H_3PO_4): δ = 54.3 ppm; IR: $\tilde{\nu}$ = 423, 479, 494, 539, 567, 660, 693, 728, 755, 819, 884, 941, 993, 1054, 1095, 1126, 1180, 1246, 1288, 1334, 1375, 1426, 1455, 1544, 1569, 2869, 2930, 2958, 3037 cm^{-1}; ESI-MS (MeCN): *m/z* (%): 476 (100) $[M]^+$; HRMS (ESI): *m/z* calcd for $C_{28}H_{49}N_2P_2^+$: 475.3365 $[M]^+$; found: 475.3368.

TiPrPN: A solution of $KN(SiMe_3)_2$ (54 mg, 0.271 mmol, 1.0 equiv) in toluene (10 mL) was added dropwise to a solution of TiPrPN·HBr (150 mg, 0.271 mmol, 1.0 equiv) in toluene (20 mL) at 0 °C. The reaction mixture was stirred for 2 h at 90 °C and filtered over celite. The filtrate was evaporated to dryness in vacuo and the remaining residue was washed with hexane to give TiPrPN as a beige solid (105 mg, 0.221 mmol, 82%). Single crystals suitable for structure determination were obtained by slowly cooling a hot saturated solution of TiPrPN in hexane to −30 °C. ^{1}H NMR (300 MHz, [D_3]MeCN, 25 °C, TMS): δ = 6.84 (t, ^3J(H,H) = 7.6 Hz, 2H, H(3,6)), 6.76 (d, ^3J(H,H) = 7.9 Hz, 2H, H(4,5)), 6.35 (dd, ^3J(H,H) = 7.3 Hz, ^4J(H,H) = 1.7 Hz, 2H, H(2,7)), 2.50 (dsept, ^3J(H,H) = 7.3 Hz, ^2J(P,H) = 11.7 Hz, 6H, H(9)), 1.22 ppm (dd, ^3J(H,H) = 7.3 Hz, ^3J(P,H) = 14.0 Hz, 36H, H(10)); ^{13}C NMR (126 MHz, [D_3]MeCN, 25 °C, TMS): δ = 154.7 (C(1,8)), 139.5 (C(4a)), 131.0 (C(8a)), 125.6 (C(3,6)), 124.4 (C(8a)), 117.3 (d, ^3J(P,C) = 8.6 Hz, C(2,7)), 116.3 (C(4,5)), 26.8 (d, ^1J(P,C) = 58.6 Hz, C(9)), 18.0 ppm (d, ^2J(P,C) = 2.6 Hz, C(10)); ^{31}P NMR (121.5 MHz, [D_3]MeCN,

25 °C, 85% H_3PO_4): $\delta = 25.6$ ppm; IR: $\tilde{\nu} = 424$, 480, 494, 536, 567, 624, 635, 660, 693, 739, 754, 772, 818, 845, 883, 929, 992, 1023, 1053, 1096, 1127, 1181, 1245, 1287, 1337, 1375, 1427, 1495, 1544, 1588, 2869, 2897, 2928, 2957, 3037 cm^{-1}; ESI-MS (MeCN): *m/z* (%): 475 (100) $[M]^+$; HRMS (ESI): *m/z* calcd for $C_{28}H_{49}N_2P_2^+$: 475.3365 $[M]^+$; found: 475.3362; elemental analysis calcd (%) for $C_{28}H_{48}N_2P_2$: C 70.85, H 5.90, N 10.19; found: C 70.88, H 6.19, N 10.36.

1,8-Bis(tricyclopentylphosphazenyl)naphthalene (TcyPPN): A solution of 1,8-diaminonaphthalene (167 mg, 1.059 mmol, 1.0 equiv) und triethylamine (429 mg, 4.236 mmol, 4.0 equiv) in chlorobenzene (10 mL) was added dropwise to a suspension of tricyclopentylbromophosphoniumbromide (843 mg, 2.117 mmol, 2.0 equiv) in chlorobenzene (30 mL). The reaction mixture was stirred for 2 h at room temperature and for additional 2 h at 80 °C. A solution of KN($SiMe_3$)$_2$ (845 mg, 4.236 mmol, 4.0 equiv) in chlorobenzene (10 mL) was added dropwise and the reaction mixture was stirred for 2 h at room temperature. The suspension was filtered over celite and the filtrate was evaporated to dryness in vacuo. The residue was extracted several times with boiling hexane (30 mL) and TcyPPN recrystallized when allowing the solution to reach room temperature. The supernatant was decanted and drying in vacuo yielded TcyPPN (373 mg, 0.591 mmol, 56%) as white crystals. ^{1}H NMR (300 MHz, [D_6]benzene, 25 °C, TMS): $\delta = 7.39$ (d, ^3J(H,H) = 8.1 Hz, 2H, H(4,5)), 7.29 (t, ^3J(H,H) = 7.5 Hz, 2H, H(3,6)), 6.83 (dd, ^3J(H,H) = 7.0 Hz, ^4J(H,H) = 2.6 Hz, 2H, H(2,7)), 2.04–1.76 (m, 18H, H(9,10)), 1.67–1.50 (m, 24H, H(10,11)), 1.67–1.50 ppm (m, 12H, H(11)); ^{13}C NMR (126 MHz, [D_6]benzene, 25 °C, TMS): $\delta = 153.9$ (C(1,8)), 138.2 (C(4a)), 133.6 (C(8a)), 124.9 (C(3,6)), 120.2 (d, ^3J(P,C) = 9.2 Hz, C(2,7)), 117.9 (C(4,5)), 38.3 (d, ^1J(P,C) = 63.6 Hz, C(9)), 28.0 (C(10)), 26.6 ppm (d, ^3J(P,C) = 9.7 Hz, C(11)); ^{31}P NMR (101 MHz, [D_6]benzene, 25 °C, 85% H_3PO_4): $\delta = 21.1$ ppm; ESI-MS (MeCN): *m/z* (%): 631 (100) $[M]^+$; HRMS (ESI): *m/z* calcd for $C_{40}H_{61}N_2P_2^+$: 631.4304 $[M]^+$; found: 631.4310; elemental analysis calcd (%) for $C_{40}H_{60}N_2P_2$: C 76.15, H 9.59, N 4.44; found: C 76.10, H 10.04, N 4.65.

TcyPPN·HPF$_6$: A solution of NH_4PF_6 (26 mg, 0.159 mmol, 1.0 equiv) in THF (6 mL) was added dropwise to a solution of TcyPPN (100 mg, 0.159 mmol, 1.0 equiv) in THF (6 mL). The precipitation of a white solid was observed after a few minutes. The suspension was stirred for 1 h at room temperature and the precipitate was separated by centrifugation and washed with pentane (15 mL). After drying in vacuo TcyPPN·HPF$_6$ (91 mg, 0.117 mmol, 74%) was obtained as a white solid.[64] ^{1}H NMR (300 MHz, [D_3]MeCN, 25 °C, TMS): $\delta = 13.34$ (t, ^2J(P,H) = 2.4 Hz, 1H, NH), 7.30 (d, ^3J(H,H) = 8.2 Hz, 2H, H(4,5)), 7.21 (t, ^3J(H,H) = 7.8 Hz, 2H, H(3,6)), 6.79 (d, ^3J(H,H) = 7.4 Hz, 2H, H(2,7)), 2.74–2.59 (m, 6H, H(9)), 1.79–1.60 ppm (m, 48H, H(10,11)); ^{13}C NMR (126 MHz, [D_3]MeCN, 25 °C, TMS): $\delta = 145.2$ (dd, ^2J(P,C) = 4.9 Hz, ^4J(P,C) = 1.5 Hz, C(1,8)), 137.2 (C(4a)), 126.9 (C(4,5)), 125.1 (t, ^3J(P,C) = 8.3 Hz, C(8a)), 121.5 (C(3,6)), 117.4 (d, ^3J(P,C) = 5.6 Hz, C(2,7)), 36.5 (d, ^1J(P,C) = 59.4 Hz, C(9)), 28.4 (C(10)), 26.5 ppm (d, ^3J(P,C) = 10.6 Hz, C(11)); ^{31}P NMR (101 MHz, [D_3]MeCN, 25 °C, 85% H_3PO_4): $\delta = 52.8$, −142.9 ppm (sept, ^1J(P,F) = 705.8 Hz, PF_6^-); ESI-MS (MeCN): *m/z* (%): 631 (100) $[M]^+$; HRMS (ESI): *m/z* calcd for $C_{40}H_{61}N_2P_2^+$: 631.4304 $[M]^+$; found: 631.4294; (−)-ESI-MS (MeCN): *m/z* (%): 145 (100) $[PF_6]^-$; HRMS ((−)-ESI): *m/z* calcd for PF_6^-: 144.9647 $[M]^-$; found: 144.9648; elemental analysis calcd (%) for $C_{40}H_{61}F_6N_2P_3$: C 61.84, H 7.91, N 3.61; found: C 61.57, H 7.99, N 3.88.

1,8-Bis(trispyrrolidinophosphazenyl)naphthalene hydrobromide (TPPN·HBr): Bromine (7.04 g, 44.04 mmol, 2.1 equiv) was added dropwise to a solution of trispyrrolidylphosphane (10.63 g, 44.04 mmol, 2.1 equiv) in benzene (200 mL) at 0 °C. Precipitation of trispyrrolidylbromophosphonium bromide was observed and the suspension was stirred for 1 h at 0 °C and for 1.5 h at room temperature. A solution of 1,8-diaminonaphthalene (3.32 g, 20.98 mmol, 1.0 equiv) and triethylamine (9.16 g, 83.89 mmol, 4.0 equiv) in benzene (50 mL) was added dropwise. The reaction mixture changed color to dark red and was stirred for 3 d at 80 °C. The hot suspension was filtered over celite and the filtrate was evaporated to dryness in vacuo. The residue was suspended in THF (100 mL) and separated from the red supernatant by filtration. The solid was washed three times with THF (25 mL) and dried in vacuo. TPPN·HBr (10.94 g, 73%) was obtained as a grey solid. ^{1}H NMR (300 MHz, [D_3]MeCN, 25 °C, TMS): $\delta = 15.02$ (br s, 1H, NH), 7.18–7.17 (m, 4H, H(2,3,4,5,6)), 6.66 (t, ^3J(H,H) = 4.4 Hz, 2H, H(2,7)), 3.26–3.21 (m, 24H, H(9)), 1.88–1.83 ppm (m, 24H, H(10)); ^{13}C NMR (76 MHz, [D_3]MeCN, 25 °C, TMS): $\delta = 144.2$ (C(1,8)), 137.7 (C(4a)), 126.9 (C(3,6)), 120.6 (t, ^3J(P,C) = 13.6 Hz, C(8a)), 120.0 (C(4,5)), 114.0 (t, ^3J(P,C) = 7.3 Hz, C(2,7)), 48.0 (d, ^2J(P,C) = 4.7 Hz, C(9)), 26.9 ppm (d, ^3J(P,C) = 8.2 Hz, C(10)); ^{31}P NMR (122 MHz, [D_3]MeCN, 25 °C, 85% H_3PO_4): $\delta = 18.1$ ppm; IR: $\tilde{\nu} = 448$, 484, 520, 548, 558, 573, 629, 650, 699, 758, 817, 872, 897, 910, 929, 954, 968, 1012, 1071, 1212, 1247, 1288, 1319, 1360, 1403, 1453, 1513, 1569, 1612, 2868, 2948, 3043 cm^{-1}; ESI-MS (MeCN): *m/z* (%): 638 (100) $[M]^+$; HRMS (ESI): *m/z* calcd for $C_{34}H_{55}N_8P_2^+$: 637.4019 $[M]^+$; found: 637.4012; elemental analysis calcd (%) for $C_{34}H_{55}BrN_8P_2$: C 56.90, H 7.72, N 15.61; found: C 55.41, H 7.69, N 15.75.

Deprotonation of TPPN·HBr: TPPN·HBr (1.500 g, 2.090 mmol, 1.0 equiv) and KN($SiMe_3$)$_2$ (0.417 g, 2.090 mmol, 1.0 equiv) were suspended in hexane (200 mL) and stirred for 24 h at 60 °C. The hot reaction mixture was filtered over celite and the filtrate was concentrated in vacuo to about 20 mL. TPPN was recrystallized at −30 °C and dried in vacuo. It was obtained as a beige solid (0.846 g, 64%). ^{1}H NMR (400 MHz, [D_3]MeCN, 25 °C, TMS): $\delta = 6.85$ (t, 2H, ^3J(H,H) = 7.7 Hz, H(3,6)), 6.69 (d, 2H, ^3J(H,H) = 7.7 Hz, H(4,5)), 6.34 (d, 2H, ^3J(H,H) = 7.7 Hz, H(2,7)), 3.23–3.19 (m, 24H, H(9)), 1.78–1.75 ppm (m, 24H, H(10)); ^{13}C NMR (101 MHz, [D_3]MeCN, 25 °C, TMS): $\delta = 153.2$ (d, ^2J(P,C) = 6.8 Hz, C(1,8)), 140.3 (t, ^3J(P,C) = 12.7 Hz, C(8a)), 128.9 (C(4a)), 126.6 (C(3,6)), 117.2 (d, ^3J(P,C) = 10.6 Hz, C(2,7)), 116.1 (C(4,5)), 48.3 (d, ^2J(P,C) = 4.5 Hz, C(9)), 27.9 ppm (d, ^3J(P,C) = 8.2 Hz, C(10)); ^{31}P NMR (122 MHz, [D_3]MeCN, 25 °C, 85% H_3PO_4): $\delta = 2.5$ ppm; IR: $\tilde{\nu} = 443$, 487, 563, 636, 748, 778, 814, 870, 912, 1005, 1065, 1125, 1195, 1239, 1290, 1341, 1383, 1430, 1544, 2858, 2957, 3039 cm^{-1}; ESI-MS (MeCN): *m/z* (%): 637 (100) $[MH]^+$, 566 (3) $[M-C_4H_8N]^+$, 497 (3) $[M-(C_4H_8N)_2]^+$, 381 (1) $[M-C_{12}H_{24}N_4P]^+$, 256 (1) $[MH^+-C_{12}H_{24}N_4P-(C_4H_8N)_2]^+$; HRMS (ESI): *m/z* calcd for $C_{34}H_{55}N_8P_2^+$: 637.4025 $[MH]^+$; found: 637.4019; elemental analysis calcd (%) for $C_{34}H_{54}N_8P_2$: C 64.13, H 8.55, N 17.60; found: C 64.16, H 8.42, N 17.57.

Bisprotonation of TPPN with HN(SO_2CF_3)$_2$: A solution of HN(SO_2CF_3)$_2$ (88 mg, 0.314 mmol, 2.0 equiv) in THF (5 mL) was added dropwise to a solution of TPPN (100 mg, 0.157 mmol, 1.0 equiv) in THF (10 mL). The reaction mixture turned to pale violet and was stirred for 1 h at room temperature. The solvent was removed in vacuo and the residue was washed with pentane (15 mL). It was dried in vacuo to obtain TPPN·2HN(SO_2CF_3)$_2$ (116 mg, 0.097 mmol, 62%) as a brown solid. ^{1}H NMR (300 MHz, [D_3]MeCN, 25 °C, TMS): $\delta = 7.85$ (d, ^3J(H,H) = 8.3 Hz, 2H, H(4,5)), 7.65 (d, ^2J(P,H) = 6.5 Hz, 2H, NH), 7.55 (t, ^3J(H,H) = 7.9 Hz, 2H, H(3,6)), 7.29 (d, ^3J(H,H) = 7.5 Hz, 2H, H(2,7)), 3.12 (dt, ^3J(H,H) = 6.7 Hz, ^3J(P,H) = 3.2 Hz, 24H, H(9)), 1.82–1.78 ppm (m, 24H, H(10)); ^{13}C NMR (101 MHz, [D_3]MeCN, 25 °C, TMS): $\delta = 137.7$ (C(4a)), 132.7 (C(1,8)), 128.0 (C(4,5)), 127.7 (C(2,7)), 124.2 (t, ^3J(P,C) = 6.0 Hz, C(8a)), 123.6 (d, ^3J(P,C) = 4.4 Hz, C(2,7)), 120.9 (quart, ^1J(C,F) = 320.8 Hz, CF_3), 48.6 (d, ^2J(P,C) = 4.9 Hz, C(9)), 26.7 ppm (d, ^3J(P,C) = 8.6 Hz, C(10)); ^{31}P NMR (101 MHz, [D_3]MeCN, 25 °C, 85% H_3PO_4): $\delta = 25.0$ ppm; ESI-MS (MeCN): *m/z* (%): 638 (100) $[M]^+$; HRMS (ESI): *m/z* calcd for $C_{34}H_{55}N_8P_2^+$:

637.4019 $[M]^+$; found: 637.4016; (−)-ESI-MS (MeCN): *m/z* (%): 280 (100) $[M]^-$; HRMS ((−)-ESI): *m/z* calcd for $C_2F_6NO_4S_2^-$: 279.9178 $[M]^-$; found: 279.9178.

Reaction of TPPN with dimethylaluminum chloride: A solution of dimethylaluminum chloride (29 mg, 0.314 mmol, 2.0 equiv) in toluene (0.8 mL) was added dropwise to a solution of TPPN (100 mg, 0.157 mmol, 1.0 equiv) in toluene (10 mL). The formation of a colorless precipitate was observed and the reaction mixture was stirred for 1 h at room temperature. The precipitate was separated by filtration and washed with pentane (20 mL). After drying in vacuo $[TPPN\text{-}AlMe_2][AlMe_2Cl_2]^-$ (111 mg, 86%) was obtained as a colorless solid. Single crystals suitable for structure determination were obtained by layering a saturated solution of $[TPPN\text{-}AlMe_2][AlMe_2Cl_2]^-$ in dichloromethane with pentane. ^{1}H NMR (300 MHz, CD_2Cl_2, 25 °C, TMS): $\delta = 7.44$ (d, $^3J(H,H) = 8.2$ Hz, 2H, H(4,5)), 7.29 (t, $^3J(H,H) = 7.8$ Hz, 2H, H(3,6)), 7.02 (dt, $^3J(H,H) = 8.0$ Hz, $^4J(H,H) = 1.5$ Hz, 2H, H(2,7)), 3.12–3.07 (m, 24H, H(9)), 1.85–1.81 (m, 24H, H(10)), −0.80 (s, 6H, AlCH_3), −0.81 ppm (s, 6H, AlCH_3); ^{31}P NMR (101 MHz, CD_2Cl_2, 25 °C, 85% H_3PO_4): $\delta = 26.3$ ppm; ESI-MS (CH_2Cl_2): *m/z* (%): 694 (100) $[M]^+$, 638 (20) $[M-AlMe_2]^+$; HRMS (ESI): *m/z* calcd for $C_{36}H_{60}AlN_8P_2^+$: 693.4226 $[M]^+$; found: 693.4223; elemental analysis calcd (%) for $C_{22}H_{42}Al_2N_2P_2$: C 55.54, H 8.09, N 13.64; found: C 55.00, H 7.79, N 13.85.

Reaction of TMPN with trimethylaluminum: A solution of trimethylaluminium (47 mg, 0.653 mmol, 2.0 equiv) in toluene (5 mL) was added dropwise to a solution of TMPN (100 mg, 0.326 mmol, 1.0 equiv) in toluene (10 mL). A white solid precipitated and the suspension was stirred for 3 h at room temperature. The precipitate was collected by filtration, washed with pentane (15 mL) and dried in vacuo. $[TMPN\text{-}AlMe_2]^+[AlMe_4]^-$ (99 mg, 67%) was obtained as a beige solid. Single crystals suitable for structure determination were obtained by layering a saturated solution of $[TMPN\text{-}AlMe_2]^+[AlMe_4]^-$ in dichloromethane with hexane. ^{1}H NMR (400 MHz, CD_2Cl_2, 25 °C, TMS): $\delta = 7.59$ (d, $^3J(H,H) = 8.3$ Hz, 2H, H(4,5)), 7.39 (t, 2H, $^3J(H,H) = 7.9$ Hz, H(3,6)), 6.88 (d, $^3J(H,H) = 7.5$ Hz, 2H, H(2,7)), 1.98 (d, $^2J(P,H) = 12.5$ Hz, 18H, H(9)), −0.86 (s, 6H, H(10)), −1.20 - −1.27 ppm (m, 12H, H(11)); ^{13}C NMR (101 MHz, CD_2Cl_2, 25 °C, TMS): $\delta = 141.3$ (d, $^2J(P,C) = 4.6$ Hz, C(1,8)), 137.4 (C(4a)), 126.5 (t, $^3J(P,C) = 8.6$ Hz, C(8a)), 126.1 (C(3,6)), 125.2 (C(4,5)), 121.0 (d, $^3J(P,C) = 10.0$ Hz, C(2,7)), 16.7 (d, $^1J(P,C) = 67.1$ Hz, C(9)), −4.6 (sext, $^1J(Al,C) = 70.5$ Hz, C(11)), −6.2 ppm (C(10)); ^{31}P NMR (101 MHz, CD_2Cl_2): $\delta = 38.5$ ppm; ESI-MS (MeCN): *m/z* (%): 307 (100) $[M-AlMe_2]^+$; HRMS (ESI): *m/z* calcd for $C_{16}H_{25}N_2P_2^+$: 307.1487 $[M-AlMe_2]^+$; found: 307.1485.

Reaction of TMPN with trimethylgallium: A solution of trimethylgallium (75 mg, 0.653 mmol, 2.0 equiv) in toluene (5 mL) was added dropwise to a solution of TMPN (100 mg, 0.326 mmol, 1.0 equiv) in toluene (10 mL). A brown solid precipitated and the suspension was stirred for 6 h at room temperature. All volatiles were removed in vacuo and the brown residue was recrystallized from dichloromethane/hexane (2:1). The precipitate was collected by filtration, washed twice with hexane (15 mL) and dried in vacuo. $[TMPN\text{-}GaMe_2]^+[GaMe_4]^-$ (68 mg, 39%) was obtained as brown needles. Single crystals suitable for structure determination were obtained by layering a saturated solution of $[TMPN\text{-}GaMe_2]^+[GaMe_4]^-$ in dichloromethane with hexane. ^{1}H NMR (400 MHz, CD_2Cl_2, 25 °C, TMS): $\delta = 7.55$ (d, $^3J(H,H) = 7.2$ Hz, 2H, H(4,5)), 7.34 (t, 2H, $^3J(H,H) = 6.9$ Hz, H(3,6)), 6.83 (d, $^3J(H,H) = 7.5$ Hz, 2H, H(2,7)), 1.84 (d, $^2J(P,H) = 12.3$ Hz, 18H, H(9)), −0.42 ppm (s, 6H, H(10)), −0.90 (s, 12H, H(11)); ^{13}C NMR (101 MHz, CD_2Cl_2, 25 °C, TMS): $\delta = 142.9$ (C(1,8)), 137.7 (C(4a)), 126.4 (t, $^3J(P,C) = 10.0$ Hz, C(8a)), 125.8 (C(3,6)), 125.0 (C(4,5)), 121.1 (d, $^3J(P,C) = 9.8$ Hz, C(2,7)), 16.7 (d, $^1J(P,C) = 67.1$ Hz, C(9)), −3.1 (C(11)), −3.4 ppm (C(10)); ^{31}P NMR (101 MHz, CD_2Cl_2, 25 °C, 85% H_3PO_4): $\delta = 38.6$ ppm; ESI-MS (MeCN): *m/z* (%): 307 (100) $[M-GaMe_2]^+$; HRMS (ESI): *m/z* calcd for $C_{16}H_{25}N_2P_2^+$: 307.1487 $[MH^+\text{-}GaMe_2]^+$; found: 307.1485; elemental analysis calcd (%) for $C_{22}H_{42}Ga_2N_2P_2$: C 49.30, H 7.90, N 5.23; found: C 48.56, H 7.96, N 5.34.

Acknowledgements

We thank Dr. Klaus Harms, Lars Finger, and Fabian Schröder for their valuable support with crystal structure refinement. Financial support by the Fonds der Chemischen Industrie (doctoral scholarship for J.K.) is gratefully acknowledged. B.K. gratefully acknowledges support of the Computing Center of the University of Zagreb (SRCE) for granting computational time on ISABELLA cluster. X.X. acknowledges the Deutsche Forschungsgemeinschaft for funding the Bruker NMR Spectrometers

Keywords: ab initio calculations · basicity · N ligands · phosphazenes

[1] P. S. Bowman, W. R. S. Steele, D. R. Winterman, R. W. Alder, *Chem. Commun. (London)* **1968**, 723–724.
[2] H. C. Brown, D. H. McDaniel, O. Häflinger in *Determination of Organic Structures by Physical Methods* (Eds.: E. A. Braude, F. C. Nachod), Academic Press, New York, **1955**, pp. 567–662.
[3] T. Ishikawa, *Superbases for organic synthesis: guanidines, amidines and phosphazenes and related organocatalysts* (Ed.: T. Ishikawa), Wiley, **2009**, pp. 251–271 and references therein.
[4] J. E. Richman, *Tetrahedron Lett.* **2010**, *51*, 2793–2796.
[5] D. A. Evans, A. M. Ratz, B. E. Huff, G. S. Sheppard, *Tetrahedron Lett.* **1994**, *35*, 7171–7172.
[6] S. Kanemasa, Y. Oderatoshi, E. Wada, *J. Am. Chem. Soc.* **1999**, *121*, 8675–8676.
[7] F. Tur, J. M. Saá, *Org. Lett.* **2007**, *9*, 5079–5082.
[8] D. Kiely, P. J. Guiry, *J. Organomet. Chem.* **2003**, *687*, 545–561.
[9] a) B. Kovačević, Z. B. Maksić, R. Vianelloa, M. Primorac, *New J. Chem.* **2002**, *26*, 1329–1334; b) A. F. Pozharskii, A. V. Degtyarev, V. A. Ozeryanskii, O. V. Ryabtsova, Z. A. Starikova, G. S. Borodkin, *J. Org. Chem.* **2010**, *75*, 4706–4715; c) A. Parkin, K. Wozniak, C. C. Wilson, *Cryst. Growth Des.* **2007**, *7*, 1393–1398; d) A. V. Degtyarev, O. V. Ryabtsova, A. F. Pozharskii, V. A. Ozeryanskii, Z. A. Starikova, L. Sobczyk, A. Filarowski, *Tetrahedron* **2008**, *64*, 6209–6214; e) C. Cox, H. Wack, T. Lectka, *Angew. Chem.* **1999**, *111*, 864–867; *Angew. Chem. Int. Ed.* **1999**, *38*, 798–800; f) V. A. Ozeryanskii, A. F. Pozharskii, A. J. Bienko, W. Sawka-Dobrowolska, L. Sobczyk, *J. Phys. Chem. A* **2005**, *109*, 1637–1642; g) J. E. Del Benea, I. Alkortab, J. Elguerob, *Magn. Reson. Chem.* **2008**, *46*, 457–463; h) A. F. Pozharskii, O. V. Ryabtsova, V. A. Ozeryanskii, A. V. Degtyarev, Z. A. Starikova, L. Sobczykc, A. Filarowskic, *Tetrahedron Lett.* **2005**, *46*, 3973–3976; i) S. M. Bachrach, *Org. Lett.* **2012**, *14*, 5598–5601; j) M. Pietrzak, J. P. Wehling, S. Kong, P. M. Tolstoy, I. G. Shenderovich, C. Lopez, R. M. Claramunt, J. Elguero, G. S. Denisov, H. Limbach, *Chem. Eur. J.* **2010**, *16*, 1679–1690; k) V. A. Ozeryanskii, A. F. Pozharskii, *Tetrahedron* **2013**, *69*, 2107–2112; l) M. T. Scerba, C. M. Leavitt, M. E. Diener, A. F. DeBlase, T. L. Guasco, M. A. Siegler, N. Bair, M. A. Johnson, T. Lectka, *J. Org. Chem.* **2011**, *76*, 7975–7984.
[10] N. C. Abacilar, V. Raab, E. Gaoutchenova, U. Garrelts, K. Harms, J. Sundermeyer, *The Chemistry of Superbasic Guanidines in Activating Unreactive Substrates, The Role of Secondary Interactions* (Eds.: C. Bolm, F. E. Hahn), Wiley-VCH, Weinheim, **2009**, pp. 17–37.
[11] a) T. Yamasaki, N. Ozaki, Y. Saika, K. Ohta, K. Goboh, F. Nakamura, M. Hashimoto, S. Okeya, *Chem. Lett.* **2004**, *33*, 928–929; b) G. Villaverde, A. Arnanz, M. Iglesias, A. Monge, F. Sanchez, N. Snejko, *Dalton Trans.* **2011**, *40*, 9589–9600; c) U. Wild, O. Hübner, A. Maronna, M. Enders, E. Kaifer, H. Wadepohl, H. Himmel, *Eur. J. Inorg. Chem.* **2008**, 4440–4447; d) V. Vitske, C. König, O. Hübner, E. Kaifer, H. Himmel, *Eur. J. Inorg. Chem.*

2010, 115 – 126; e) S. Wiesner, A. Ziesak, M. Reinmuth, P. Walter, E. Kaifer, H. Wadepohl, H. Himmel, *Eur. J. Inorg. Chem.* **2013**, 163 – 171.

[12] a) R. Shroff, A. Svatoš, *Anal. Chem.* **2009**, *81*, 7954 – 7959; b) R. Shroff, A. Svatoš, *Rapid Commun. Mass Spectrom.* **2009**, *23*, 2380 – 2382; c) S. Zhang, Z.-P. Yao, *Anal. Chim. Acta* **2012**, *711*, 77 – 82; d) C. D. Calvano, C. G. Zambonin, F. Palmisano, *Rapid Commun. Mass Spectrom.* **2011**, *25*, 1757 – 1764; e) D. Cao, Z. Wang, C. Han, L. Cui, M. Hu, J. Wu, Y. Liu, Y. Cai, H. Wang, Y. Kang, *Talanta* **2011**, *85*, 345 – 352; f) C. D. Calvano, A. Monopoli, N. Ditaranto, F. Palmisano, *Anal. Chim. Acta* **2013**, *798*, 56 – 63.

[13] D. Cao, M. Hu, C. Han, J. Yu, L. Cui, Y. Liu, H. Wang, Y. Cai, Y. Kang, Y. Zhou, *Analyst* **2012**, *137*, 2218 – 2225.

[14] Y. Zou, PhD Thesis, Universität Stuttgart (Germany), **2001**.

[15] R. E. Cherpeck, C. Y. Chan, G. Bhalla (Chevron Oronite Company), CA 2646839, **2008**.

[16] a) R. W. Alder, N. C. Goode, N. Miller, F. Hibbert, K. P. P. Hunte, H. J. Robbins, *J. Chem. Soc. Chem. Commun.* **1978**, *3*, 89 – 90; b) R. W. Alder, M. R. Bryce, N. C. Goode, N. Miller, J. Owen, *J. Chem. Soc. Perkin Trans. 1* **1981**, 2840 – 2847; c) F. Hibbert, K. P. P. Hunte, *J. Chem. Soc. Perkin Trans. 2* **1983**, 1895 – 1890; d) A. F. Pozharskii, O. V. Ryabtsova, V. A. Ozeryanskii, A. V. Degtyarev, O. N. Kazheva, G. G. Alexandrov, O. A. Dyachenko, *J. Org. Chem.* **2003**, *68*, 10109 – 10122; e) A. V. Degtyarev, A. F. Pozharskii, *Chem. Heterocycl. Compd.* **2008**, *44*, 1138 – 1145; f) E. A. Filatova, A. F. Pozharskii, A. V. Gulevskaya, N. V. Vistorobskii, V. A. Ozeryanskii, *Synlett* **2013**, *24*, 2515 – 2518.

[17] F. J. Hibbert, *Chem. Soc. Perkin Trans. 2* **1974**, 1862 – 1866.

[18] A. Awwal, F. J. Hibbert, *Chem. Soc. Perkin Trans. 2* **1977**, 1589 – 1592.

[19] F. Hibbert, G. R. Simpson, *J. Chem. Soc. Perkin Trans. 2* **1987**, 613 – 615.

[20] M. A. Zirnstein, H. A. Staab, *Angew. Chem.* **1987**, *99*, 460 – 461; *Angew. Chem. Int. Ed. Engl.* **1987**, *26*, 460 – 461.

[21] K. J. Shaffer, D. C. Parr, M. Wenzel, G. J. Rowlands, P. G. Plieger, *Eur. J. Org. Chem.* **2012**, 6967 – 6975.

[22] H. A. Staab, T. Saupe, C. Krieger, *Angew. Chem.* **1983**, *95*, 748 – 749; *Angew. Chem. Int. Ed. Engl.* **1983**, *22*, 731 – 732.

[23] H. A. Staab, M. Höne, C. Krieger, *Tetrahedron Lett.* **1988**, *29*, 1905 – 1908.

[24] T. Saupe, C. Krieger, H. A. Staab, *Angew. Chem.* **1986**, *98*, 460 – 462; *Angew. Chem. Int. Ed. Engl.* **1986**, *25*, 451 – 453.

[25] H. A. Staab, C. Krieger, M. Hone, *Tetrahedron Lett.* **1988**, *29*, 5629 – 5632.

[26] H. A. Staab, M. A. Zirnstein, C. Krieger, *Angew. Chem.* **1989**, *101*, 73 – 75; *Angew. Chem. Int. Ed. Engl.* **1989**, *28*, 86 – 88.

[27] H. Zachova, S. Man, J. Taraba, M. Potacek, *Tetrahedron* **2009**, *65*, 792 – 797; b) J. Galeta, M. Potáček, *J. Org. Chem.* **2012**, *77*, 1010 – 1017.

[28] a) I. Despotović, B. Kovačević, Z. B. Maksić, *Org. Lett.* **2007**, *9*, 4709 – 4712; b) S. M. Bachrach, C. C. Wilbanks, *J. Org. Chem.* **2010**, *75*, 2651 – 2660; c) N. Uchida, J. Kuwabara, A. Taketoshi, T. Kanbara, *J. Org. Chem.* **2012**, *77*, 10631 – 10637.

[29] L. Belding, T. Dudding, *Chem. Eur. J.* **2014**, *20*, 1032 – 1037.

[30] R. Schwesinger, H. Schlemper, *Angew. Chem.* **1987**, *99*, 1210 – 1212; *Angew. Chem. Int. Ed. Engl.* **1987**, *26*, 1165 – 1167.

[31] a) V. Raab, J. Kipke, R. M. Gschwind, J. Sundermeyer, *Chem. Eur. J.* **2002**, *8*, 1682 – 1693; b) V. Raab, K. Harms, J. Sundermeyer, B. Kovačević, Z. B. Maksić, *J. Org. Chem.* **2003**, *68*, 8790 – 8797.

[32] R. Schwesinger, H. Schlemper, C. Hasenfratz, J. Willaredt, T. Dambacher, T. Breuer, C. Ottaway, M. Fletschinger, J. Boele, H. Fritz, D. Putzas, H. W. Rotter, F. G. Brodwell, A. V. Satish, G. Ji, E. Peters, K. Peters, H. G. von Schnering, L. Walz, *Liebigs Ann.* **1996**, *7*, 1055 – 1081 and references therein.

[33] V. Raab, E. Gauchenova, A. Merkoulov, K. Harms, J. Sundermeyer, B. Kovačević, Z. B. Maksić, *J. Am. Chem. Soc.* **2005**, *127*, 15738 – 15743.

[34] J. F. Kögel, B. Oelkers, B. Kovačević, J. Sundermeyer, *J. Am. Chem. Soc.* **2013**, *135*, 17768 – 17774.

[35] a) H. A. Staab, T. Saupe, *Angew. Chem.* **1988**, *100*, 895 – 909; *Angew. Chem. Int. Ed. Engl.* **1988**, *27*, 865 – 879; b) R. W. Alder, *Chem. Rev.* **1989**, *89*, 1215 – 1223; c) A. L. Llamas-Saiz, C. Foces-Foces, J. Elguero, *J. Mol. Struct.* **1994**, *328*, 297 – 323; d) Z. B. Maksić, B. Kovačević, R. Vianello, *Chem. Rev.* **2012**, *112*, 5240 – 5270; e) A. F. Pozharskii, *Russ. Chem. Rev.* **1998**, *67*, 1 – 24; f) A. F. Pozharskii, V. A. Ozeryanskii, E. A. Filatova, *Chem. Heterocycl. Compd.* **2012**, *48*, 200 – 219; g) J. Chambron, M. Meyer, *Chem. Soc. Rev.* **2009**, *38*, 1663 – 1673.

[36] a) A. L. Llamas-Saiz, C. Foces-Foces, P. Molina, M. Alajarin, A. Vidal, R. M. Claramunt, J. Elguero, *J. Chem. Soc. Perkin Trans. 2* **1991**, 1025 – 1031; b) A. L. Llamas-Saiz, C. Foces-Foces, J. Elguero, P. Molina, M. Alajarin, A. Vidal, *J. Chem. Soc. Perkin Trans. 2* **1991**, 1667 – 1676; c) A. L. Llamas-Saiz, C. Foces-Foces, J. Elguero, P. Molina, M. Alajarin, A. Vidal, *J. Chem. Soc. Perkin Trans. 2* **1991**, 2033 – 2040; d) J. Laynez, M. Menendez, S. Velasco, J. Luis, A. L. Llamas-Saiz, C. Foces-Foces, J. Elguero, P. Molina, M. Alajarin, A. Vidal, *J. Chem. Soc. Perkin Trans. 2* **1993**, 709 – 713.

[37] H. G. Alt, K. J. Schneider, E. Funk, *Jord. J. Chem.* **2008**, *3*, 367 – 379.

[38] TBPN has been known in our group since 2011 (E. Baal, bachelor thesis, Philipps-Universität Marburg (Germany), **2011**) and was presented at the ESOR XIII (J. F. Kögel, B. Oelkers, B. Kovačević, Z. B. Maksić, J. Sundermeyer, "New Superbasic Bisphosphazene Proton Sponges", 13th European Symposium on Organic Reactivity (ESOR XIII), Tartu, 11.–16.09.2011).

[39] a) Y. Xiong, S. Yao, S. Inoue, A. Berkefeld, M. Driess, *Chem. Commun.* **2012**, *48*, 12198 – 12200; b) Y. Xiong, S. Yao, S. Inoue, E. Irran, M. Driess, *Angew. Chem.* **2012**, *124*, 10221 – 10224; *Angew. Chem.* **2012**, *124*, 10221 – 10224; *Angew. Chem. Int. Ed. Angew. Chem. Int. Ed. Engl.* **2012**, *51*, 10074 – 10077.

[40] H. Staudinger, J. Meyer, *Helv. Chim. Acta* **1919**, *2*, 635 – 646.

[41] a) A. V. Kirsanov, *Izv. Akad. Nauk SSSR, Otd. Khim. Nauk* **1950**, 426; b) G. I. Derkach, I. N. Zhmurova, A. V. Kirsanov, V. I. Shevchenko, A. S. Shtepanek, *Phosphazo Compounds* **1965**, Naukova Dumka, Kiew.

[42] J. F. Kögel, N. C. Abacılar, F. Weber, B. Oelkers, K. Harms, B. Kovačević, J. Sundermeyer, *Chem. Eur. J.* **2014**, manuscript accepted, 201304498.

[43] T. Rodima, V. Mäemets, I. Koppel, *J. Chem. Soc. Perkin Trans. 1* **2000**, 2637 – 2644.

[44] We prepared up to 10.94 g TPPN·HBr from the described procedure. In principle, further upscaling should be possible.

[45] The crystal structure of TMPN·HBr contained half a unit of NH_4Br per unit of TMPN·HBr. The structure was prepared from the protonation reaction of crude TMPN with NH_4PF_6. The used TMPN contained traces of TMPN·HBr leading to crystallization of the hydrobromide instead of the HPF_6 salt. It was verified by bromide analysis that the bulk of TMPN·HPF_6 was free of bromide.

[46] The molecular structure of TBPN·HBr has already been published in the Supporting Information of ref. [39b]. The synthesis of TBPN·HBr is described in the Supporting Information.

[47] *d*(NH) was restrained at 0.85 Å in case of TPPN·$HN(SO_2CF_3)_2$ and therefore is not discussed herein.

[48] See ref. [11a].

[49] a) M. Reinmuth, U. Wild, D. Rudolf, E. Kaifer, M. Enders, H. Wadepohl, H.-J. Himmel, *Eur. J. Inorg. Chem.* **2009**, 4795 – 4808; b) P. Roquette, A. Maronna, A. Peters, E. Kaifer, H.-J. Himmel, C. Hauf, V. Herz, E.-W. Scheidt, W. Scherer, *Chem. Eur. J.* **2010**, *16*, 1336 – 1350; c) A. Maronna, E. Bindewald, E. Kaifer, H. Wadepohl, H.-J. Himmel, *Eur. J. Inorg. Chem.* **2011**, 1302 – 1314; d) V. Vitske, P. Roquette, S. Leingang, C. Adam, E. Kaifer, H. Wadepohl, H.-J. Himmel, *Eur. J. Inorg. Chem.* **2011**, 1593 – 1604.

[50] a) H.-U. Wüstefeld, W. C. Kaska, F. Schüth, G. D. Stuckly, X. Bu, B. Krebs, *Angew. Chem.* **2001**, *113*, 3280 – 3282; *Angew. Chem. Int. Ed.* **2001**, *40*, 3182 – 3184; b) H.-U. Wuestefeld, W. C. Kaska, G. D. Stucky, F. Schueth, B. Krebs, PCT Int. Appl., WO 2002059134 A1 20020801, **2002;** c) K. J. Shaffer, M. Wenzel, P. G. Plieger, *Polyhedron* **2013**, *52*, 1399 – 1402.

[51] a) R. R. Ernst, G. Bodenhausen, A. Wokaun, *Principles of Nuclear Magnetic Resonance in One and Two Dimensions*, Oxford University Press, London/New York, **1987**; b) C. L. Perrin, T. J. Dwyer, *Chem. Rev.* **1990**, *90*, 935 – 967.

[52] S. Berger, S. Braun, *200 and More NMR Experiments, a Practical Course*, Wiley-VCH, Weinheim, **2004**.

[53] Gaussian 03, Revision E.01, M. J. Frisch, G. W. Trucks, H. B. Schlegel, G. E. Scuseria, M. A. Robb, J. R. Cheeseman, J. A. Montgomery, Jr., T. Vreven, K. N. Kudin, J. C. Burant, J. M. Millam, S. S. Iyengar, J. Tomasi, V. Barone, B. Mennucci, M. Cossi, G. Scalmani, N. Rega, G. A. Petersson, H. Nakatsuji, M. Hada, M. Ehara, K. Toyota, R. Fukuda, J. Hasegawa, M. Ishida, T. Nakajima, Y. Honda, O. Kitao, H. Nakai, M. Klene, X. Li, J. E. Knox, H. P. Hratchian, J. B. Cross, V. Bakken, C. Adamo, J. Jaramillo, R. Gomperts, R. E. Stratmann, O. Yazyev, A. J. Austin, R. Cammi, C. Pomelli, J. W. Ochterski, P. Y. Ayala, K. Morokuma, G. A. Voth, P. Salvador, J. J. Dannenberg, V. G. Zakrzewski, S. Dapprich, A. D. Daniels, M. C. Strain, O. Farkas, D. K. Malick, A. D. Rabuck, K. Raghavachari, J. B. Foresman, J. V. Ortiz, Q. Cui, A. G. Baboul, S. Clifford, J. Cioslowski, B. B. Stefanov, G. Liu, A. Liashenko, P. Piskorz, I. Komaromi, R. L. Martin, D. J. Fox, T. Keith, M A. Al-

Laham, C. Y. Peng, A. Nanayakkara, M. Challacombe, P. M. W. Gill, B. Johnson, W. Chen, M. W. Wong, C. Gonzalez, J. A. Pople, Gaussian, Inc., Wallingford CT, **2004**.

[54] B. Kovačević, D. Barić, Z. B. Maksić, *New J. Chem.* **2004**, *28*, 284 – 288.

[55] S. T. Howard, *J. Am. Chem. Soc.* **2000**, *122*, 8238 – 8244.

[56] V. C. Gibson, C. E. Graimann, P. M. Hare, M. L. H. Green, J. A. Bandy, P. D. Grebenik, K. Prout, *J. Chem. Soc. Dalton Trans.* **1985**, 2025 – 2035.

[57] W. C. Davies, *J. Chem. Soc.* **1933**, 1043 – 1044.

[58] D. J. Dellinger, D. M. Sheehan, N. K. Christensen, J. G. Lindberg, M. H. Caruthers, *J. Am. Chem. Soc.* **2003**, *125*, 940 – 950.

[59] R. Bartsch, O. Stelzer, R. Schmutzler, *Z. Naturforsch. B* **1981**, *36*, 1349 – 1355.

[60] G. Brauer, *Handbuch der Präparativen Anorganischen Chemie, 3. Auflage*, Ferdinand Enke Verlag, Stuttgart, **1975**, pp. 712 – 713.

[61] J. Ahman, P. Somfai, *Synth. Commun.* **1995**, *25*, 2301 – 2303.

[62] Single crystals suitable for structure determination of protonated TBPN were obtained by layering a saturated solution of TBPN·HBr in THF with hexane. The preparation of the hydrobromide is described in the Supporting Information.

[63] The origin of this coupling constant could not be identified.

[64] Single crystals suitable for structure determination of protonated TcyPPN were obtained by diffusion of pentane into a saturated solution of TcyPPN·HBr in chlorobenzene. The preparation of the hydrobromide is described in the Supporting Information.

[65] CCDC-997546 (TMPN·HBr), -997546 (TBPN·HBr), -997548 (TiPrPN·HBr), -997550 (TcyPPN·HBr), -997549 (TiPrPN), -997551 (TcyPPN), -997553 ($[TMPN\text{-}AlMe_2]^+[AlMe_4]^-$), -997554 ($[TMPN\text{-}GaMe_2]^+[GaMe_4]^-$), and -997552 ($[TPPN\text{-}AlMe_2]^+[AlCl_2Me_2]^-$), contain the supplementary crystallographic data for this paper. These data can be obtained free of charge from The Cambridge Crystallographic Data Centre via www.ccdc.cam.ac.uk/data_request/cif.

Received: February 17, 2014
Published online on May 5, 2014